



First excursion probability sensitivity in stochastic linear dynamics by means of Domain Decomposition Method

Mauricio A. Misraji *, Marcos A. Valdebenito , Matthias G.R. Faes

Chair for Reliability Engineering, TU Dortmund University, Leonhard-Euler-Straße 5, 44227 Dortmund, Germany

ARTICLE INFO

Communicated by S. Fassois

Keywords:

First excursion probability
Sensitivity analysis
Gaussian loading
Linear structure
Domain Decomposition Method

ABSTRACT

This contribution introduces a novel framework for the first excursion probability sensitivity estimation, applicable to linear dynamic systems subject to Gaussian excitation. The sensitivity estimator considered here is a local one and is calculated as the partial derivative of the first excursion probability with respect to a design parameter, such as the geometrical dimensions of the system. In the context of stochastic dynamical systems with low failure probability, obtaining both reliability and sensitivity estimates can be computationally expensive. In that sense, the linearity of the system plays a key role in order to build an efficient estimator. Domain Decomposition Method exploits this feature by exploring the failure domain in a very convenient way due to its special structure, characterized by the union of a large number of elementary linear failure domains. The proposed approach is based on the Domain Decomposition Method, enabling the derivation of the sensitivity estimator as a byproduct of the first excursion probability estimator. The effectiveness of the presented technique is illustrated through numerical examples involving both small- and large-scale models.

1. Introduction

The dynamic analysis of mechanical and structural systems is commonly carried out with numerical models. Due to the unavoidable effects of uncertainty, it is highly challenging to perform the system analysis under the traditional approach, which is based on deterministic concepts. Nowadays, the theory of random vibrations offers tools to incorporate the uncertainty in several engineering problems [1]. For example, the effects of uncertainty associated with earthquakes and wind loads on structures, or the effect of atmospheric turbulence on airplanes, can be assessed with a reliability analysis. Indeed, the so-called first excursion probability allows quantifying the system's reliability under one or more performance criteria, for instance, if a response of interest exceeds a predefined threshold during the stochastic loading. In cases where the system's behavior remains linear, the first excursion probability can provide a measure with respect to a serviceability criterion [2–4]. Consequently, various advanced simulation methods have been developed to calculate the first excursion probability by leveraging the linearity of the system. These methods include, for example, a very Efficient Importance Sampling (EIS) [5], Domain Decomposition Method (DDM) [6], Directional Importance Sampling (DIS) [7], and lastly, multidomain Line Sampling (mLS) [8].

The first excursion probability can be affected considerably due to changes in structural properties, such as alterations in mass, stiffness, or geometrical dimensions of structural members. In particular, considering nonproportional damping in the system is of utmost importance, as it provides a more realistic representation of dynamic behavior compared to proportional damping [9]. This generalized approach of the system differs from the cases considered in, e.g. [10,11]. Therefore, studying the sensitivity of the first

* Corresponding author.

E-mail address: mauricio.misraji@tu-dortmund.de (M.A. Misraji).

<https://doi.org/10.1016/j.ymssp.2025.112865>

Received 28 October 2024; Received in revised form 6 May 2025; Accepted 13 May 2025

Available online 7 June 2025

0888-3270/© 2025 The Authors. Published by Elsevier Ltd. This is an open access article under the CC BY license (<http://creativecommons.org/licenses/by/4.0/>).

excursion probability is fundamental to achieve a more exhaustive reliability assessment [12–16]. This information can be used, in the context of risk evaluation [17], decision making [18], as well as reliability-based design optimization problems [19].

The sensitivity of the first excursion probability can be calculated in terms of its gradient, which corresponds to a local measure (that is, how the probability changes due to small perturbations in structural properties). Nevertheless, the aforementioned calculation usually demands solving a high dimensional integral that does not possess a closed-form solution. This problem has been explored in the literature in the past [20–24], where two different classes of cases can be distinguished [25]. The first one is the calculation of the gradient with respect to distribution parameters of random variables, which are considered to represent the uncertainty associated with some structural properties [26,27]. The second class includes those problems where the gradient of the probability is calculated with respect to deterministic parameters affecting the structural behavior. This group includes approaches that combines the use of Bayes' theorem with stochastic simulation for the sensitivity estimates calculation [28,29], approaches which consider second-order moments approximations [30], and approaches that combine stochastic simulation with local approximations of the responses of interest [10,31,32].

An approach that is particularly useful to estimate first-excursion probabilities is the so-called Domain Decomposition Method. This contribution proposes a novel framework to extend the application of this method towards estimating the sensitivity of the first excursion probability applied to small- and large-scale finite element models. The work is focused on linear structural systems with either nonproportional or proportional damping, subjected to a Gaussian loading. The analysis focuses on local sensitivity, which is derived by computing the partial derivatives of the first excursion probability with respect to each deterministic design parameter. Moreover, the sensitivity estimator is achieved as a byproduct of the reliability analysis [33] together with a sensitivity analysis of the spectral properties of the system [34]. The use of Domain Decomposition Method plays a key role in the failure domain exploration. This is due to its particular structure, which is a union of a large number of linear elementary failure domains. Additionally, the incorporation of an Importance Sampling density function [11] allows the estimation of the sensitivity of the first excursion probability with a reduced number of samples.

The next sections of this contribution are organized as follows. Section 2 presents the problem, the first excursion probability and its gradient definition. Section 3 presents the aforementioned gradient calculation by means of Domain Decomposition Method. Then, two examples of the proposed framework are illustrated in Section 4. Finally, Section 5 draws the discussion to a close and presents thoughts on future developments.

2. Problem statement

This section defines the theoretical framework of the problem addressed in this work. The stochastic loading is presented in Section 2.1, while the system definition and the responses of interest are detailed in Section 2.2. Section 2.3 introduces the first excursion probability problem, and Section 2.4 presents its sensitivity analysis. Finally, Section 2.5 describes the special geometric structure of the failure domain.

2.1. Gaussian loading

The dynamic load p acting on the system is described as a discrete Gaussian process of duration T , discretized in n_T times instants of duration Δt . Accordingly, the k -time instant is defined as $t_k = (k-1)\Delta t, k = 1, \dots, n_T$. The expected value of this process at time t_k is defined as μ_k , which is the k th element of the expected value vector $\boldsymbol{\mu}$ of dimension $n_T \times 1$. The covariance matrix associated with the Gaussian loading is $\boldsymbol{\Sigma}$. It is symmetric, bounded and positive definite, where the covariance between times t_{k_1} and t_{k_2} is given by Σ_{k_1, k_2} , corresponding to the (k_1, k_2) th element of $\boldsymbol{\Sigma}$. The dynamic load is represented in terms of the Karhunen–Loève expansion as [35,36]

$$p(t_k, \mathbf{z}) = \mu_k + \boldsymbol{\Psi}_k^T \mathbf{z}, \quad k = 1, \dots, n_T, \quad (1)$$

where $p(t_k, \mathbf{z})$ is the loading at time t_k and \mathbf{z} is a realization of a standard Gaussian random variable vector \mathbf{Z} of dimensions $n_{KL} \times 1$, being n_{KL} the order of truncation of the expansion ($n_{KL} \leq n_T$). By solving the eigenproblem $\boldsymbol{\Sigma} \boldsymbol{\Xi} = \boldsymbol{\Xi} \boldsymbol{\Lambda}$ associated with the largest n_{KL} eigenvalues of $\boldsymbol{\Sigma}$, the set of vectors $\boldsymbol{\Psi} = [\boldsymbol{\Psi}_1, \boldsymbol{\Psi}_2, \dots, \boldsymbol{\Psi}_{n_T}]$ can be calculated as $\boldsymbol{\Psi} = \boldsymbol{\Lambda}^{1/2} \boldsymbol{\Xi}^T$, being $\boldsymbol{\Psi}_k, k = 1, \dots, n_T$ a vector of dimensions $n_{KL} \times 1$ related to the time instant t_k . In this work, it is assumed the specific case where $\boldsymbol{\mu} = \mathbf{0}$ without loss of generality.

2.2. Structural system

The system is considered linear elastic and damped, and is subject to a Gaussian loading $p(t, \mathbf{z})$. Moreover, the system is composed by n_D degrees-of-freedom and is governed by the following equation of motion [37]:

$$\mathbf{M}(\mathbf{y})\ddot{\mathbf{x}}(t, \mathbf{y}, \mathbf{z}) + \mathbf{C}(\mathbf{y})\dot{\mathbf{x}}(t, \mathbf{y}, \mathbf{z}) + \mathbf{K}(\mathbf{y})\mathbf{x}(t, \mathbf{y}, \mathbf{z}) = \mathbf{g}(\mathbf{y})p(t, \mathbf{z}), \quad t \in [0, T], \quad (2)$$

where the displacement, velocity and acceleration are represented by \mathbf{x} , $\dot{\mathbf{x}}$ and $\ddot{\mathbf{x}}$, respectively, all vectors of dimension $n_D \times 1$; the matrices of mass \mathbf{M} , damping \mathbf{C} and stiffness \mathbf{K} are of dimensions $n_D \times n_D$; the coupling vector of the loading with the degrees of freedom of the system is \mathbf{g} , which has dimensions $n_D \times 1$; and the deterministic vector that contains the parameters which

represent the structural properties of the system is \mathbf{y} , of dimension $n_Y \times 1$. To address the general case of structural systems exhibiting nonproportional damping, Eq. (2) may be reformulated into the following augmented system [38]:

$$\begin{bmatrix} \mathbf{0}_{n_D \times n_D} & \mathbf{M}(\mathbf{y}) \\ \mathbf{M}(\mathbf{y}) & \mathbf{C}(\mathbf{y}) \end{bmatrix} \begin{Bmatrix} \dot{\mathbf{x}}(t, \mathbf{y}, \mathbf{z}) \\ \mathbf{x}(t, \mathbf{y}, \mathbf{z}) \end{Bmatrix} + \begin{bmatrix} -\mathbf{M}(\mathbf{y}) & \mathbf{0}_{n_D \times n_D} \\ \mathbf{0}_{n_D \times n_D} & \mathbf{K}(\mathbf{y}) \end{bmatrix} \begin{Bmatrix} \dot{\mathbf{x}}(t, \mathbf{y}, \mathbf{z}) \\ \mathbf{x}(t, \mathbf{y}, \mathbf{z}) \end{Bmatrix} = \begin{Bmatrix} \mathbf{0}_{n_D \times 1} \\ \mathbf{g}(\mathbf{y}) \end{Bmatrix} p(t, \mathbf{z}), \quad (3)$$

or in its compact form:

$$[\mathbf{M}_a(\mathbf{y})] \{\dot{\mathbf{q}}(t, \mathbf{y}, \mathbf{z})\} + [\mathbf{K}_a(\mathbf{y})] \{\mathbf{q}(t, \mathbf{y}, \mathbf{z})\} = \{\mathbf{g}_a(\mathbf{y})\} p(t, \mathbf{z}), \quad (4)$$

where \mathbf{q} is a vector grouping velocities and displacements of the system, with dimensions $2n_D \times 1$, \mathbf{M}_a and \mathbf{K}_a are the augmented mass and stiffness matrices of dimensions $2n_D \times 2n_D$, respectively, and \mathbf{g}_a is the augmented load coupling vector of dimensions $2n_D \times 1$, with the augmented matrices and vectors defined explicitly as:

$$[\mathbf{M}_a(\mathbf{y})] = \begin{bmatrix} \mathbf{0}_{n_D \times n_D} & \mathbf{M}(\mathbf{y}) \\ \mathbf{M}(\mathbf{y}) & \mathbf{C}(\mathbf{y}) \end{bmatrix}; \quad [\mathbf{K}_a(\mathbf{y})] = \begin{bmatrix} -\mathbf{M}(\mathbf{y}) & \mathbf{0}_{n_D \times n_D} \\ \mathbf{0}_{n_D \times n_D} & \mathbf{K}(\mathbf{y}) \end{bmatrix};$$

$$\{\mathbf{g}_a(\mathbf{y})\} = \begin{Bmatrix} \mathbf{0}_{n_D \times 1} \\ \mathbf{g}(\mathbf{y}) \end{Bmatrix}; \quad \{\mathbf{q}(t, \mathbf{y}, \mathbf{z})\} = \begin{Bmatrix} \dot{\mathbf{x}}(t, \mathbf{y}, \mathbf{z}) \\ \mathbf{x}(t, \mathbf{y}, \mathbf{z}) \end{Bmatrix}. \quad (5)$$

It is paramount to control some dynamical responses, such as displacements, accelerations, internal stresses, as well their linear combinations. These responses are defined as $\eta_i(t, \mathbf{y}, \mathbf{z})$, $i = 1, \dots, n_\eta$, and is calculated using the convolution integral [37]:

$$\eta_i(t, \mathbf{y}, \mathbf{z}) = \int_0^t h_i(t - \tau, \mathbf{y}) p(\tau, \mathbf{z}) d\tau, \quad i = 1, \dots, n_\eta, \quad (6)$$

where $h_i(t, \mathbf{y})$, $i = 1, \dots, n_\eta$ is the unit impulse function of the i th response of interest, and $p(t, \mathbf{z})$ corresponds to the Gaussian loading. Eq. (6) is deduced assuming null initial conditions, that is $\mathbf{x}(0, \mathbf{y}, \mathbf{z}) = \dot{\mathbf{x}}(0, \mathbf{y}, \mathbf{z}) = \mathbf{0}_{n_D \times 1}$. Therefore, when the response of interest is a combination of the vector $\mathbf{q}(t, \mathbf{y}, \mathbf{z})$, it can be expressed as $\eta_i(t, \mathbf{y}, \mathbf{z}) = \boldsymbol{\gamma}_i^T \mathbf{q}(t, \mathbf{y}, \mathbf{z})$, where $\boldsymbol{\gamma}_i$ is a constant vector of dimension $2n_D \times 1$. Then, the unit impulse response function associated to the i th response of interest is written as [39]:

$$h_i(t, \mathbf{y}) = \sum_{r=1}^{2n_D} \frac{\boldsymbol{\gamma}_i^T \boldsymbol{\phi}_r(\mathbf{y}) \boldsymbol{\phi}_r(\mathbf{y})^T \mathbf{g}_a(\mathbf{y})}{\boldsymbol{\phi}_r(\mathbf{y})^T \mathbf{M}_a(\mathbf{y}) \boldsymbol{\phi}_r(\mathbf{y})} e^{\lambda_r(\mathbf{y})t}, \quad i = 1, \dots, n_\eta, \quad (7)$$

where $\boldsymbol{\phi}_r(\mathbf{y})$ and $\lambda_r(\mathbf{y})$ are the eigenvectors and eigenvalues associated with the eigenproblem of Eq. (4). It is worth noting that, in cases where the system involves a large number of degrees of freedom, it is convenient to apply modal truncation [37] to Eq. (7) by selecting a number of modes smaller than $2n_D$. Given the discretized definition of the Gaussian loading in time as discussed in Section 2.1, it is possible to approximate the integral associated with the response of interest integral mentioned in Eq. (6) at specific time instant t_k as:

$$\eta_i(t_k, \mathbf{y}, \mathbf{z}) = \mathbf{a}_{i,k}(\mathbf{y})^T \mathbf{z}, \quad i = 1, \dots, n_\eta, \quad k = 1, \dots, n_T, \quad (8)$$

where the vector $\mathbf{a}_{i,k}(\mathbf{y})$ of dimension $n_{KL} \times 1$ is defined as:

$$\mathbf{a}_{i,k}(\mathbf{y}) = \sum_{m=1}^k \Delta t \epsilon_m h_i(t_k - t_m, \mathbf{y}) \boldsymbol{\psi}_m, \quad (9)$$

where ϵ_m depends on the preferred integration scheme, for example, with a trapezoidal scheme $\epsilon_m = 1/2$ for $m = 1, k$ and otherwise $\epsilon_m = 1$ [40]. It is worth mentioning that in Eq. (8) the dependence of the design vector \mathbf{y} is only related to $\mathbf{a}_{i,k}$, and in the same way, the dependence of the vector \mathbf{z} is only related to the Gaussian load p .

2.3. First excursion probability

The design requirements are defined by the vector \mathbf{b} of dimension $n_\eta \times 1$, where b_i is its i th element, and correspond to the prescribed threshold for the response of interest η_i . The performance function $g(\mathbf{y}, \mathbf{z})$ indicates if the response of interest η_i exceeds or not a prescribed threshold b_i along the duration of the excitation, and is given by:

$$g(\mathbf{y}, \mathbf{z}) = 1 - \max_{i=1, \dots, n_\eta} \left(\max_{k=1, \dots, n_T} \left(\frac{|\eta_i(t_k, \mathbf{y}, \mathbf{z})|}{b_i} \right) \right), \quad (10)$$

where $|\cdot|$ is the absolute value. Furthermore, the failure domain can be formally defined as $F = \{\mathbf{z} \in \mathbb{R}^{n_{KL}} : g(\mathbf{y}, \mathbf{z}) \leq 0\}$.

The probability associated with the failure domain can be quantified by means of the so-called first excursion probability [1]:

$$p_F(\mathbf{y}) = \int_{g(\mathbf{y}, \mathbf{z}) \leq 0} f_Z(\mathbf{z}) d\mathbf{z}, \quad (11)$$

where $f_Z(\mathbf{z})$ is the standard Gaussian probability density function in n_{KL} dimensions.

For practical engineering applications n_{KL} can be relatively large, in the order of hundreds or thousands. As a consequence, the first excursion probability shown in Eq. (11) becomes a high dimensional integral which does not have a closed-form solution and must be evaluated with advanced simulation methods [41]. This challenge has led to the development of advanced simulation methods that leverage the system's linearity to estimate the first excursion probability [5–8].

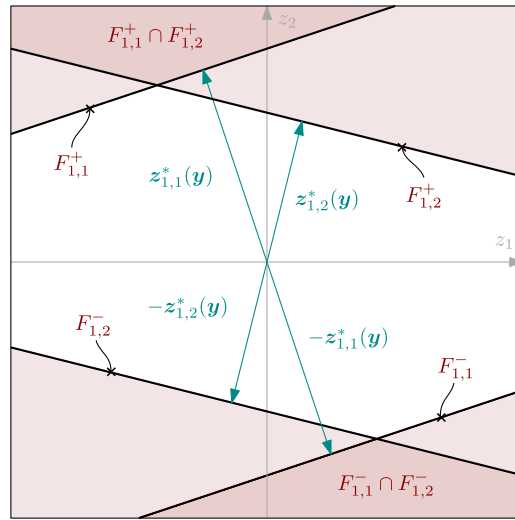


Fig. 1. Elementary failure domains representation for the case where $n_\eta = 1$ and $n_T = n_{KL} = 2$.

2.4. Gradient of first excursion probability

The dependence of the first excursion probability on the design parameters vector \mathbf{y} , highlights the importance of studying the sensitivity of Eq. (11). One potential approach to measure that sensitivity is calculating the gradient of the first excursion probability, as follows (see Appendix A):

$$\frac{\partial p_F(\mathbf{y})}{\partial y_q} = - \int_{g(\mathbf{y}, \mathbf{z})=0} \frac{\partial g(\mathbf{y}, \mathbf{z})}{\partial y_q} \frac{1}{\|\nabla_{\mathbf{z}} g(\mathbf{y}, \mathbf{z})\|} f_{\mathbf{Z}}(\mathbf{z}) dS, \quad q = 1, \dots, n_y, \tag{12}$$

where $\|\cdot\|$ denotes Euclidean norm; $\nabla_{\mathbf{z}}$ is the nabla operator $\nabla_{\mathbf{z}} = [\partial/\partial z_1, \dots, \partial/\partial z_{n_{KL}}]^T$; and dS denotes a differential element of the limit state hypersurface $S = \{\mathbf{z} \in \mathbb{R}^{n_{KL}} : g(\mathbf{y}, \mathbf{z}) = 0\}$. Evaluation of the expression in Eq. (12) poses a significant challenge, as it comprises solving a $(n_{KL} - 1)$ -dimensional integral over a hypersurface and the calculation of derivatives of the performance function.

2.5. Geometry of the failure domain

The failure domain for a linear dynamical system that is subject to Gaussian loading has a very special geometry, which can be defined analytically in the standard Gaussian space [5,42]. To understand how the failure domain mentioned in Section 2.3 is constructed, from Eq. (10), it is straightforward noting that the failure domain can be decomposed in $n_\eta \times n_T$ elementary failure domains. Each of them, denoted as $F_{i,k}$, describes the event where the response η_i exceeds the prescribed threshold b_i at the time instant t_k , which can be also decomposed in its positive and negative sides, which means that $F_{i,k} = F_{i,k}^+ \cup F_{i,k}^-$. Then, the elementary failure domain that represents if the response of interest η_i exceeding its threshold b_i at the time instant t_k is defined as $F_{i,k}^+ = \{\mathbf{z} \in \mathbb{R}^{n_{KL}} : \mathbf{a}_{i,k}^T(\mathbf{y})\mathbf{z} \geq b_i\}$. In a similar manner, the elementary failure domain that represents if the response of interest $-\eta_i$ exceeding its threshold b_i at the time instant t_k is defined as $F_{i,k}^- = \{\mathbf{z} \in \mathbb{R}^{n_{KL}} : \mathbf{a}_{i,k}^T(\mathbf{y})\mathbf{z} \leq -b_i\}$. Now, the failure domain is defined as the union of all the elementary failure domains, that is $F = \bigcup_{i=1}^{n_\eta} \bigcup_{k=1}^{n_T} F_{i,k}$. Following the same logic, it is also possible to define the performance function associated to the i th response of interest at the k th time instant as $g_{i,k}(\mathbf{y}, \mathbf{z})$, being its positive part denoted as $g_{i,k}^+(\mathbf{y}, \mathbf{z})$ and its negative part denoted as $g_{i,k}^-(\mathbf{y}, \mathbf{z})$. A schematic representation of the elementary failure domains is shown in Fig. 1, for the case where $n_\eta = 1$ and $n_T = n_{KL} = 2$. It is possible to observe that the positive and negative parts of the elementary failure domains $F_{1,1}$ and $F_{1,2}$ are illustrated, as well as the interaction between them. In this context, interaction is understood as the event where both of the elementary failure domains $F_{1,1}$ and $F_{1,2}$ occur, meaning that the response of interest exceeds its prescribed threshold at both time instants. This two-dimensional representation of the problem gives an idea of the degree of overlapping existing between the elementary failure domains when the problem involves a large number of dimensions.

Focusing on one elementary failure domain, the realization of \mathbf{z} that has the highest likelihood is the one with the smallest Euclidean norm from the origin [5,42], which is the so-called design point. It allows to define analytically the elementary failure domain, and is given by:

$$\mathbf{z}_{i,k}^*(\mathbf{y}) = b_i \frac{\mathbf{a}_{i,k}(\mathbf{y})}{\|\mathbf{a}_{i,k}(\mathbf{y})\|^2}, \quad i = 1, \dots, n_\eta, \quad k = 1, \dots, n_T. \tag{13}$$

where $\mathbf{z}_{i,k}^*$ (\mathbf{y}) is the design point associated to the $F_{i,k}^+$ elementary failure domain. The Euclidean norm of the design point, known as the reliability index, is equal to:

$$\beta_{i,k}(\mathbf{y}) = \frac{b_i}{\|\mathbf{a}_{i,k}(\mathbf{y})\|}, \quad i = 1, \dots, n_\eta, \quad k = 1, \dots, n_T, \quad (14)$$

being the reliability index $\beta_{i,k}(\mathbf{y})$ associated to the elementary failure domain $F_{i,k}$. Therefore, from the definition of the elementary failure domain, it is evident that the probability of occurrence $P[F_{i,k}^+] = P[F_{i,k}^-] = \Phi[-\beta_{i,k}]$, where $P[\cdot]$ denotes probability and $\Phi[\cdot]$ corresponds to the one-dimensional Gaussian cumulative density function. Then, the summation of the probability of occurrence of all the elementary failure domains independently is given by:

$$\hat{p}_F = \sum_{i=1}^{n_\eta} \sum_{k=1}^{n_T} P[F_{i,k}] = 2 \sum_{i=1}^{n_\eta} \sum_{k=1}^{n_T} \Phi(-\beta_{i,k}), \quad (15)$$

where \hat{p}_F represents an upper bound for the first excursion probability p_F [5].

3. Sensitivity estimation of first excursion probability

This section presents the methodology for estimating the first excursion probability and its sensitivity using the Domain Decomposition Method. Section 3.1 contextualizes the proposed method within the scope of the formulated problem. In Section 3.2, the Domain Decomposition Method is formulated for estimating the first excursion probability. Section 3.3 develops the sensitivity estimation procedure. Section 3.4 addresses practical implementation aspects, including the differentiation of key terms. Finally, Section 3.5 summarizes the procedure for computing both reliability and sensitivity estimators.

3.1. General remarks

For several simulation-based methods, gradient estimation typically becomes a post-process of the reliability analysis [21,24,27]. Given their applicability to a wide range of engineering problems [12,17–19], it makes sense to obtain both estimators, despite the additional computational cost.

The first excursion probability sensitivity integral evaluation, as shown in Eq. (12), requires performing integration over the limit state hypersurface. This quantity can be estimated using various simulation schemes. For instance, literature suggests that this task can be accomplished through Directional Sampling [43] and Line Sampling [33]. When the failure domain has a particular structure, as shown in Eq. (10), it is possible to perform this task in a more sophisticated manner, with the novelty of this work relying on the latter.

A framework based on Domain Decomposition Method [6] is chosen to estimate both the failure probability and its sensitivity. For this purpose, the failure probability integral is expressed in terms of the *effective contribution* of each elementary failure domain, followed by a mathematical development involving Directional Sampling [43] and Importance Sampling [44], yielding the same first excursion probability estimators as shown in [6]. Note that the deduction for the Domain Contribution Method presented here (see Section 3.2) differs from the one originally presented in [6]. Such alternative deduction is chosen on purpose, as it facilitates the calculation of the probability sensitivity, as discussed in Section 3.3.

3.2. Domain decomposition method

3.2.1. Effective contribution of the elementary failure domains

The particular geometry of the failure domain defined in Section 2.5 gives substantial information of the analytical definition of the elementary failure domains. Moreover, it is evident from Fig. 1 that there may be overlapping between the elementary failure domains. In the context of high-dimensional problems, the degree of overlap may be significant, which consequently complicates the estimation of the first excursion probability. To address this issue, leveraging the elementary failure domain definition, the failure probability integral defined in Eq. (11) can be written in terms of the contribution of each of the individual elementary failure domains [5,8], which is given by:

$$p_F(\mathbf{y}) = \sum_{i=1}^{n_\eta} \sum_{k=1}^{n_T} p_{i,k}(\mathbf{y}), \quad (16)$$

where $p_{i,k}(\mathbf{y})$ is termed as *effective contribution* associated with the elementary failure domain $F_{i,k}$, which is defined as follows:

$$p_{i,k}(\mathbf{y}) = \int_{\mathbf{z} \in F_{i,k}} \frac{1}{\sum_{h=1}^{n_\eta} \sum_{j=1}^{n_T} I_{F_{h,j}}(\mathbf{y}, \mathbf{z})} f_Z(\mathbf{z}) d\mathbf{z}, \quad (17)$$

where $I_{F_{h,j}}(\mathbf{y}, \mathbf{z})$ is an indicator function which is equal to 1 in case that $\mathbf{z} \in F_{i,k}$. The *discounting factor* $1 / \sum_{h=1}^{n_\eta} \sum_{j=1}^{n_T} I_{F_{h,j}}(\mathbf{y}, \mathbf{z})$ accounts for discounting the effective contribution resulting from the interaction between elementary failure domains. To understand the effective contribution definition, consider the calculation of the effective contribution $p_{1,2}$ from the example presented in Fig. 1. The elementary failure domain associated with $F_{1,2}$ can be separated into two regions: the domain $F_2 \setminus (F_1 \cap F_2)$, which is a region without overlap, and the domain $F_{1,2} \cap F_{1,1}$, which is a region with overlap. Then, considering a possible realization \mathbf{z} of \mathbf{Z} , the

Table 1
Inner integral decomposition of Eq. (18) and effective contribution discounting factor in example shown in Fig. 2.

Segment	$1/\sum_{h=1}^{n_\eta} \sum_{j=1}^{n_T} I_{F_{h,j}}(\mathbf{y}, r\mathbf{u})$
$[c_{1,3}(\mathbf{y}, \mathbf{u}), c_{1,2}(\mathbf{y}, \mathbf{u})[$	–
$[c_{1,2}(\mathbf{y}, \mathbf{u}), c_{1,1}(\mathbf{y}, \mathbf{u})[$	2
$[c_{1,1}(\mathbf{y}, \mathbf{u}), \infty[$	3

discounting factor $1/\sum_{h=1}^{n_\eta} \sum_{j=1}^{n_T} I_{F_{h,j}}(\mathbf{y}, \mathbf{z})$ becomes 1 if $\mathbf{z} \in F_2 \setminus (F_1 \cap F_2)$, and 1/2 if $\mathbf{z} \in F_{1,2} \cap F_{1,1}$. Repeating the process for the calculation of $p_{1,1}$, and the calculation of p_F by using Eq. (16), it is straightforward to note that the contribution to the failure probability of the region with overlap is considered, with one half accounted for in the calculation of $p_{1,1}$ and the other half in the calculation of $p_{1,2}$. This implies that the effective contribution $p_{i,k}$ corresponds to the probability of occurrence of the event $F_{i,k}$, reduced by the discounting factor due to the overlap between elementary failure domains.

3.2.2. Reliability

The estimation of the failure probability shown in Eq. (11) is done by estimating the effective contribution of the elementary failure domains. In order to achieve this, Eq. (17) is written using the Directional Sampling scheme [43,45,46]. This technique allows writing the realization vector \mathbf{z} in terms of its Euclidean norm r and its unitary direction \mathbf{u} , that means $\mathbf{z} = r\mathbf{u}$. The unit vector is defined in the standard Gaussian space and is calculated as $\mathbf{u} = \mathbf{z}/\|\mathbf{z}\|$ and the Euclidean norm is defined as $r = \|\mathbf{z}\|$, where r^2 follows a Chi-squared distribution of n_{KL} degrees-of-freedom [47]. Therefore, the resulting effective contribution integral is reformulated as:

$$p_{i,k}(\mathbf{y}) = \int_{\mathbf{u} \in \Omega_U} \int_{r\mathbf{u} \in F_{i,k}} \frac{2rf_{R^2}(r^2) f_U(\mathbf{u})}{\sum_{h=1}^{n_\eta} \sum_{j=1}^{n_T} I_{F_{h,j}}(\mathbf{y}, r\mathbf{u})} dr d\mathbf{u}, \tag{18}$$

where $\Omega_U = \{\mathbf{u} \in \mathbb{R}^{n_{KL}} : \mathbf{u}^T \mathbf{u} = 1\}$ denotes the sample space for \mathbf{u} ; $f_U(\mathbf{u})$ corresponds to the uniform probability density function over the $(n_{KL} - 1)$ -dimensional hypersphere; and $f_{R^2}(\cdot)$ is the Chi-squared probability density function with n_{KL} degrees of freedom. It is possible to demonstrate [47] that the term $2rf_{R^2}(r^2)$ arises from transforming the probability distribution associated with r to the Chi-squared probability distribution, which depends on r^2 .

For a better understanding of the discounting factor in the context of Directional Sampling, Fig. 2 illustrates the case with $n_\eta = 1$, $n_T = 3$, and $n_{KL} = 2$ when estimating $p_{1,2}$. For simplicity, only the positive side of the elementary failure domains are labeled. It is worth noting that, from Eq. (18), the inner integral (highlighted with the green arrow in Fig. 2) given a realization of the unit direction vector \mathbf{u} , has an analytical solution due to the system's linearity. Indeed, it can be solved by decomposing its integration interval into segments, where in each of these segments, exhibits a different degree of overlap between elementary failure domains. In other words, the integration interval is subdivided into parts where the discounting factor $1/\sum_{h=1}^{n_\eta} \sum_{j=1}^{n_T} I_{F_{h,j}}(\mathbf{y}, r\mathbf{u})$ from Eq. (18) remains constant. Therefore, in order to define the intervals for the integral, the following definition is considered:

$$c_{i,k}(\mathbf{y}, \mathbf{u}) = \frac{b_i}{\eta_i(t_k, \mathbf{y}, r\mathbf{u})}, \tag{19}$$

where $c_{i,k}(\mathbf{y}, \mathbf{u})$ corresponds to the Euclidean distance from the origin pointing in \mathbf{u} direction to the intersection with the elementary failure domain $F_{i,k}$. For instance, in Fig. 2, given a direction \mathbf{u} , the ray extending from the origin intersects three elementary failure domains as it extends to infinity along the coordinate r . The corresponding distances are $c_{1,3}$, $c_{1,2}$, and $c_{1,1}$, respectively. Then, by decomposing the integral interval, the resulting values, along with the discounting factor for each segment, are presented in Table 1. Note that even though the failure domain includes the event $F_{1,3}$, the integration is performed within the domain of $F_{1,2}$ when calculating the effective contribution $p_{1,2}$.

In order to improve the readability of the solution to inner integral of Eq. (18), a sorted notation using the index l is introduced. The objective is that given a unit direction \mathbf{u} , the elementary failure domains that intersect the ray extending from the origin to infinity (along the coordinate r) can be sorted in increasing order of their Euclidean distances. Therefore, the vector that contains the sorted elementary failure domains $\mathbf{F}(\mathbf{u})$ can be written in terms of the index l as:

$$\mathbf{F}(\mathbf{u}) = [F_l, F_{l+1}, F_{l+2}, \dots, F_{n_l(\mathbf{u})}]^T, \tag{20}$$

where $l \in [1, \dots, n_l(\mathbf{u})]$, being $n_l(\mathbf{u})$ the maximum number of intersections with elementary failure domains in the unit direction \mathbf{u} , which is lower or equal than $n_\eta \times n_T$. Nevertheless, the calculation of the effective contribution $p_{i,k}$ requires performing the integration over the failure domain $F_{i,k}$, as is shown in Eq. (24). In turn, the inner integral must be evaluated over the coordinate r , which is defined from the boundary of the $F_{i,k}$ elementary failure domain to infinity. As a consequence, for each effective contribution $p_{i,k}$, it is necessary to find the value of the index l , which is associated with the failure domain $F_{i,k}$. For simplicity and without loss of generality, this value is defined as L for a given direction \mathbf{u} , which represents the L th position of the elementary failure domain $F_{i,k}$ in the sorted vector $\mathbf{F}(\mathbf{u})$ defined in Eq. (20). In order to understand the notation introduced, Fig. 3 and Table 2 represents the situation, while calculating $p_{1,2}$. It is possible to note that the intersection between the elementary failure domains and the ray that starts from the origin and extends to infinity in the direction of \mathbf{u} occurs in the following order: $F_{1,3}$, $F_{1,2}$, and $F_{1,1}$. Thus, with the

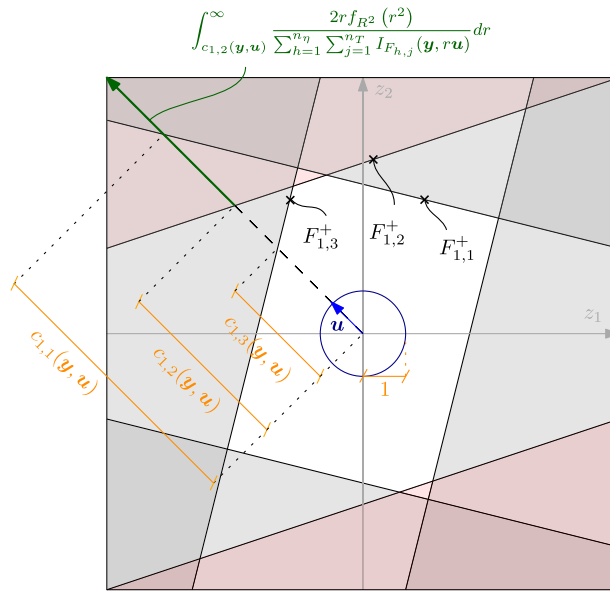


Fig. 2. Inner integral of Eq. (18) in the context of $p_{1,2}$ estimation for the case where $n_\eta = 1$, $n_T = 3$ and $n_{KL} = 2$.

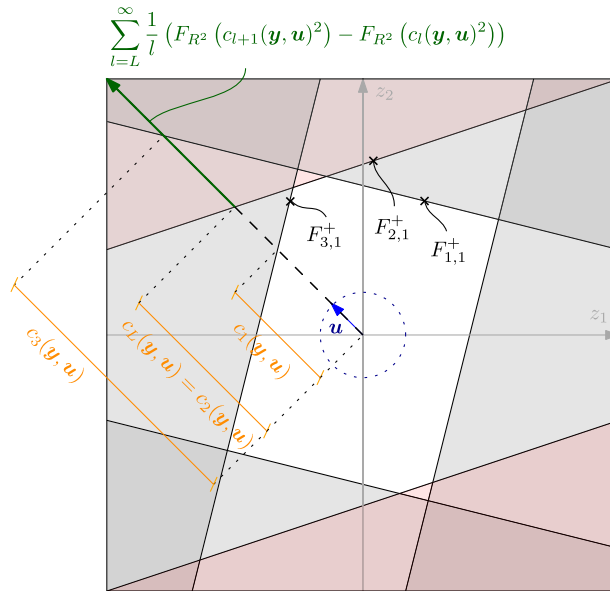


Fig. 3. Inner integral of Eq. (18) in the context of $p_{1,2}$ estimation, using the sorted notation for the case where $n_\eta = 1$, $n_T = 3$ and $n_{KL} = 2$.

sorted notation, these elementary failure domains become F_1 , F_2 , and F_3 respectively. The same idea applies to the c -distances. The inner integral in Eq. (24) is represented by the green arrow, indicating that the lower bound corresponds to c_L , where $L = 2$ in this case. Therefore, implementing the sorted notation and by solving the inner integral of Eq. (24), the expression becomes:

$$\int_{c_L}^{\infty} \frac{2rf_{R^2}(r^2) f_U(\mathbf{u})}{\sum_{h=1}^{n_\eta} \sum_{j=1}^{n_T} I_{F_{h,j}}(\mathbf{y}, r\mathbf{u})} dr = \sum_{l=L}^{\infty} \frac{1}{l} (F_{R^2}(c_{l+1}(\mathbf{y}, \mathbf{u})^2) - F_{R^2}(c_l(\mathbf{y}, \mathbf{u})^2)), \tag{21}$$

being the term $1/l$ equivalent to the discounting factor $1/\sum_{h=1}^{n_\eta} \sum_{j=1}^{n_T} I_{F_{h,j}}(\mathbf{y}, r\mathbf{u})$ from the integral in Eq. (18), and $F_{R^2}(\cdot)$ is the Chi-squared cumulative density function with n_{KL} degrees of freedom.

The calculation of a single effective contribution also involves solving the outer integral of Eq. (18). This integration can be estimated through simulation methods, such as Monte Carlo simulation, by generating random samples of \mathbf{u} . However, this method may not be efficient within the context of high-dimensional problems and small failure probabilities estimation, due to the number

Table 2
c-distances associated to Fig. 3 given a direction \mathbf{u} .

r value	Intersected domain	Sorted notation		
		Index l	r value using index l	Intersected domain using index l
$c_{1,3}$	$F_{1,3}$	1	c_1	F_1
$c_{1,2}$	$F_{1,2}$	2	$c_2 = c_L$	F_2
$c_{1,1}$	$F_{1,1}$	3	c_3	F_3

of dynamic analyses required to get a robust estimator. To address this issue, a more efficient approach based on Importance Sampling [44] is used, by introducing an importance sampling probability density function $f_U^{IS}(\mathbf{u})$. Therefore, Eq. (18) can be written as:

$$p_{i,k}(\mathbf{y}) = \int_{\mathbf{u} \in \Omega_U} \sum_{l=L}^{\infty} \frac{1}{l} (F_{R^2}(c_{l+1}(\mathbf{y}, \mathbf{u})^2) - F_{R^2}(c_l(\mathbf{y}, \mathbf{u})^2)) \frac{f_U(\mathbf{u})}{f_U^{IS}(\mathbf{u})} f_U^{IS}(\mathbf{u}) d\mathbf{u}. \quad (22)$$

The importance sampling density function $f_U^{IS}(\mathbf{u})$ is based on [5,7], with the difference that each effective contribution $p_{i,k}$ has its own importance sampling density function. It is defined as the probability density associated with the direction \mathbf{u} conditioned on the occurrence of an elementary failure event $F_{i,k}$ (see Appendix B for further details). Then, the importance sampling density function, associated to the (i, k) th effective contribution, is written as:

$$f_U^{IS,(i,k)}(\mathbf{u}) = f_U(\mathbf{u} | F_{i,k}). \quad (23)$$

Then, by using the definitions from Eqs. (22) and (23), the effective contribution $p_{i,k}$ becomes:

$$p_{i,k}(\mathbf{y}) = P[F_{i,k}] \int_{\mathbf{u} \in \Omega_U} \lambda_{i,k}(\mathbf{y}, \mathbf{u}) f_U^{IS,(i,k)}(\mathbf{u}) d\mathbf{u}, \quad (24)$$

with

$$\lambda_{i,k}(\mathbf{y}, \mathbf{u}) = \sum_{l=L}^{\infty} \frac{1}{l} \frac{F_{R^2}(c_{l+1}(\mathbf{y}, \mathbf{u})^2) - F_{R^2}(c_l(\mathbf{y}, \mathbf{u})^2)}{1 - F_{R^2}(c_L(\mathbf{y}, \mathbf{u})^2)}. \quad (25)$$

Theoretically, solving the integral of Eq. (24) by integrating over all the directions \mathbf{u} , the effective contribution $p_{i,k}$ can be expressed as:

$$p_{i,k}(\mathbf{y}) = P[F_{i,k}] \bar{\lambda}_{i,k}(\mathbf{y}), \quad (26)$$

where $\bar{\lambda}_{i,k}(\mathbf{y})$ is given by:

$$\bar{\lambda}_{i,k}(\mathbf{y}) = \int_{\mathbf{u} \in \Omega_U} \lambda_{i,k}(\mathbf{y}, \mathbf{u}) f_U^{IS,(i,k)}(\mathbf{u}) d\mathbf{u}. \quad (27)$$

The term $\bar{\lambda}_{i,k}(\mathbf{y})$ can be interpreted as a compensation for the overlapping existing between the elementary failure domain $F_{i,k}$ and others, which is pondered over all the directions where $\{\mathbf{r}\mathbf{u} \in F_{i,k}\}$. It is straightforward to note that the definition presented in Eq. (26) is equivalent to the one presented in Eq. (17), with a more convenient construction of the discounting factor. Therefore, Eq. (26) provides an expression for calculating the effective contribution $p_{i,k}$ within the framework of *Domain Decomposition Method*.

However, the calculation of the failure probability using Eq. (16) requires determining each effective contribution $p_{i,k}$, where $i = 1, \dots, n_\eta$ and $k = 1, \dots, n_T$. This can be extremely demanding due to the product $n_\eta \times n_T$, which could be on the order of hundreds or thousands. To address this challenge, the summation in Eq. (16) can be estimated using simulation, as in [6]. Then, considering an alternative to Eq. (16) as:

$$p_F(\mathbf{y}) = \sum_{i=1}^{n_\eta} \sum_{k=1}^{n_T} \left(\frac{1}{w_{i,k}} p_{i,k}(\mathbf{y}) \right) w_{i,k}, \quad (28)$$

where $w_{i,k}$ is the weight considered in the importance sampling density of Eq. (23) and is defined in Appendix B, which serves as a probability mass function. Therefore, the expression in Eq. (28) involves a summation over a discrete random variable $w_{i,k}$ and an integration over a continuous random variable \mathbf{u} . This can be solved through simulation by generating samples of both random variables, as follows:

$$p_F(\mathbf{y}) \approx \bar{p}_F(\mathbf{y}) = \frac{1}{N} \sum_{j=1}^N \left(\frac{1}{w_{(i,k)^{(j)}}} \bar{p}_{(i,k)^{(j)}}(\mathbf{y}, \mathbf{u}_{(i,k)^{(j)}}) \right), \quad (29)$$

where \bar{p}_F corresponds to an estimate of p_F ; N is the total number of samples; $(i, k)^{(j)}$, $j = 1, \dots, N$, are independent and identically distributed samples chosen from the set $I = \{1, \dots, n_\eta \times n_T\}$ with probability mass function $w_{i,k}$, where $i = 1, \dots, n_\eta$ and $k = 1, \dots, n_T$; the vector $\mathbf{u}_{(i,k)^{(j)}}$ is distributed according to $f_U^{IS,(i,k)}(\mathbf{u})$; and $\bar{p}_{(i,k)^{(j)}}(\mathbf{u}_{(i,k)^{(j)}})$ is the estimate of the effective contribution $p_{i,k}(\mathbf{u})$

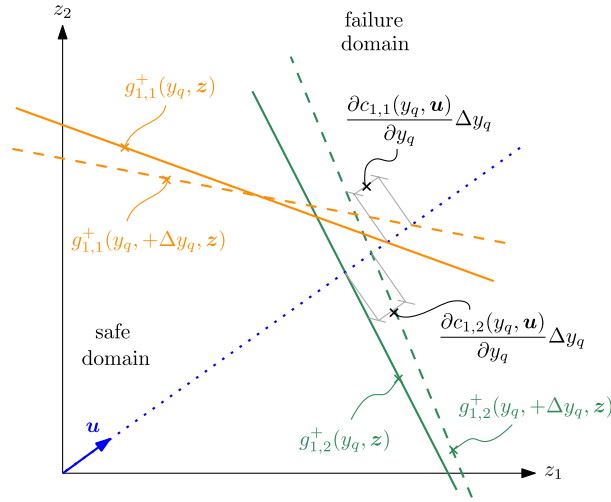


Fig. 4. Schematic representation for the sensitivity of the effective contributions for the case where $n_y = 1$, $n_T = n_{KL} = 2$ and $n_y = 1$.

evaluated at the sample $\mathbf{u}_{(i,k)j}$. To estimate the effective contribution, it is necessary to estimate the term $\bar{\lambda}_{i,k}(\mathbf{y})$ by evaluating the sampled direction $\mathbf{u}_{(i,k)j}$ in Eq. (25), which means:

$$\bar{p}_{(i,k)j}(\mathbf{y}, \mathbf{u}_{(i,k)j}) \approx P[F_{i,k}] \lambda_{i,k}(\mathbf{y}, \mathbf{u}_{(i,k)j}) = P[F_{i,k}] \sum_{l=L}^{\infty} \frac{1}{l} \frac{F_{R^2}(c_{l+1}(\mathbf{y}, \mathbf{u}_{(i,k)j}))^2 - F_{R^2}(c_l(\mathbf{y}, \mathbf{u}_{(i,k)j}))^2}{1 - F_{R^2}(c_l(\mathbf{y}, \mathbf{u}_{(i,k)j}))^2} \quad (30)$$

Eq. (29) yields the first excursion probability estimator using the *Domain Decomposition Method*. It is worth noting that the result is the same as that presented in [6] with an alternative deduction.

Finally, it can be easily proven that the coefficient of variation δ_{p_F} of the first excursion probability estimator in Eq. (29) is equal to:

$$\delta_{p_F} = \frac{1}{\bar{p}_F(\mathbf{y})} \sqrt{\frac{1}{N(N-1)} \sum_{j=1}^N \left(\left(\frac{1}{w_{(i,k)j}} \bar{p}_{(i,k)j}(\mathbf{y}, \mathbf{u}_{(i,k)j}) \right) - \bar{p}_F(\mathbf{y}) \right)^2} \quad (31)$$

3.3. Sensitivity

The estimation of the sensitivity of the first excursion probability shown in Eq. (12) can be performed by estimating the derivative of the effective contributions, from Eq. (17), with respect to a design parameter y_q , resulting as follows:

$$\frac{\partial p_F(\mathbf{y})}{\partial y_q} = \sum_{i=1}^{n_y} \sum_{k=1}^{n_T} \frac{\partial p_{i,k}(\mathbf{y})}{\partial y_q}, \quad (32)$$

where $\partial p_{i,k}(\mathbf{y})/\partial y_q$ denotes the partial derivative of the effective contribution $p_{i,k}(\mathbf{y})$ with respect the design parameter y_q . To exemplify the changes in the effective contribution due to a change in the design parameter, consider the schematic two-dimensional representation shown in Fig. 4, for the case where $n_y = 1$, $n_T = n_{KL} = 2$ and $n_y = 1$, in the context of calculating $p_{1,1}$. For simplicity, only the positive elementary failure domains are presented. The limit state function associated with the elementary failure domain $F_{1,1}^+$ (with the orange line) is given by $g_{1,1}^+(y_q, z)$, and the one associated with the elementary failure domain $F_{1,2}^+$ (with the green line) is given by $g_{1,2}^+(y_q, z)$. After introducing a change Δy_q to the design parameter y_q , the limit state functions become $g_{1,1}^+(y_q + \Delta y_q, z)$ and $g_{1,2}^+(y_q + \Delta y_q, z)$, respectively. The sensitivity of the effective contributions represents the quantification of the potential change between the overlapping between the elementary failure domains due to a change in the design parameter. It is worth noting that in the context of estimating the effective contribution $p_{1,2}$ through direction \mathbf{u} , the distance $c_{1,2}$ changes by $(\partial c_{1,2}(y_q, \mathbf{u})/\partial y_q)\Delta y_q$, and the distance $c_{1,1}$ changes by $(\partial c_{1,1}(y_q, \mathbf{u})/\partial y_q)\Delta y_q$ while using Eq. (30).

The partial derivative of the effective contribution in Eq. (32) can be calculated using Leibniz' rule [48]. Therefore, from Eqs. (18) and (21), and using the sorted notation introduced in Section 3.2.2, this derivative can be expressed as:

$$\frac{\partial p_{i,k}(\mathbf{y})}{\partial y_q} = \int_{\mathbf{u} \in \Omega_U} \sum_{l=L}^{\infty} \frac{1}{l} \frac{\partial}{\partial y_q} (F_{R^2}(c_{l+1}(\mathbf{y}, \mathbf{u}))^2 - F_{R^2}(c_l(\mathbf{y}, \mathbf{u}))^2) f_U(\mathbf{u}) d\mathbf{u}. \quad (33)$$

Note from Eq. (33) that only the c -distances depend on the design parameter. Therefore, the derivative of the effective contribution is given by:

$$\frac{\partial p_{i,k}(\mathbf{y})}{\partial y_q} = \int_{\mathbf{u} \in \Omega_U} \sum_{l=L}^{\infty} \frac{1}{l} \left(2c_{l+1}(\mathbf{y}, \mathbf{u}) \frac{\partial c_{l+1}(\mathbf{y}, \mathbf{u})}{\partial y_q} f_{R^2}(c_{l+1}(\mathbf{y}, \mathbf{u})^2) - 2c_l(\mathbf{y}, \mathbf{u}) \frac{\partial c_l(\mathbf{y}, \mathbf{u})}{\partial y_q} f_{R^2}(c_l(\mathbf{y}, \mathbf{u})^2) \right) f_U(\mathbf{u}) d\mathbf{u}, \tag{34}$$

where $f_{R^2}(\cdot)$ is the Chi-squared probability density function with n_{KL} degrees of freedom, and $\partial c_l(\mathbf{y}, \mathbf{u})/\partial y_q$ is the partial derivative of $c_l(\mathbf{y}, \mathbf{u})$ with respect to the design parameter y_q (its calculation is discussed in Section 3.4).

Following the same idea as in Section 3.2.2, calculating all the derivatives of the effective contribution from Eq. (32) requires a significant computational effort. To address this issue, an importance sampling density function can be introduced, resulting in:

$$\frac{\partial p_{i,k}(\mathbf{y})}{\partial y_q} = \int_{\mathbf{u} \in \Omega_U} \sum_{l=L}^{\infty} \frac{1}{l} \left(2c_{l+1}(\mathbf{y}, \mathbf{u}) \frac{\partial c_{l+1}(\mathbf{y}, \mathbf{u})}{\partial y_q} f_{R^2}(c_{l+1}(\mathbf{y}, \mathbf{u})^2) - 2c_l(\mathbf{y}, \mathbf{u}) \frac{\partial c_l(\mathbf{y}, \mathbf{u})}{\partial y_q} f_{R^2}(c_l(\mathbf{y}, \mathbf{u})^2) \right) \frac{f_U(\mathbf{u})}{f_U^{IS}(\mathbf{u})} f_U^{IS}(\mathbf{u}) d\mathbf{u}. \tag{35}$$

The importance sampling density function is chosen similarly for both reliability and sensitivity analyses, using Eq. (23). Although this function is primarily designed to improve the efficiency of the reliability estimator calculation, it also serves as a convenient choice for calculating sensitivity estimates as a byproduct of the reliability analysis. Using the definition in Eqs. (23) and (35), the sensitivity of the effective contribution can be written as:

$$\frac{\partial p_{i,k}(\mathbf{y})}{\partial y_q} = P[F_{i,k}] \int_{\mathbf{u} \in \Omega_U} \mu_{i,k}(\mathbf{y}, \mathbf{u}) f_U^{IS,(i,k)}(\mathbf{u}) d\mathbf{u}, \tag{36}$$

where

$$\mu_{i,k}(\mathbf{y}, \mathbf{u}) = \sum_{l=L}^{\infty} \frac{1}{l(1 - F_{R^2}(c_l^2))} \left(2c_{l+1}(\mathbf{y}, \mathbf{u}) \frac{\partial c_{l+1}(\mathbf{y}, \mathbf{u})}{\partial y_q} f_{R^2}(c_{l+1}(\mathbf{y}, \mathbf{u})^2) - 2c_l(\mathbf{y}, \mathbf{u}) \frac{\partial c_l(\mathbf{y}, \mathbf{u})}{\partial y_q} f_{R^2}(c_l(\mathbf{y}, \mathbf{u})^2) \right). \tag{37}$$

Assuming that the derivative is defined over all possible directions $\mathbf{u} \in \Omega_U$, if theoretically the integral of Eq. (36) is solved, the derivative of the effective contribution can be expressed as:

$$\frac{\partial p_{i,k}(\mathbf{y})}{\partial y_q} = P[F_{i,k}] \bar{\mu}_{i,k}(\mathbf{y}), \tag{38}$$

where $\bar{\mu}_{i,k}(\mathbf{y})$ is given by:

$$\bar{\mu}_{i,k}(\mathbf{y}) = \int_{\mathbf{u} \in \Omega_U} \mu_{i,k}(\mathbf{y}, \mathbf{u}) f_U^{IS,(i,k)}(\mathbf{u}) d\mathbf{u}. \tag{39}$$

Therefore, Eq. (38) provides an expression for calculating the derivative of the effective contribution $p_{i,k}$ with respect to a design parameter y_q within the framework of *Domain Decomposition Method*.

However, the calculation of the failure probability using Eq. (32) requires determining each of the derivatives of the effective contribution $\partial p_{i,k}(\mathbf{y})/\partial y_q$, where $i = 1, \dots, n_\eta$ and $k = 1, \dots, n_T$. This can be extremely demanding due to the product $n_\eta \times n_T$, which could be on the order of hundreds or thousands. To address this issue, the summation in Eq. (32) can be estimated through simulation, in the same manner as the reliability analysis shown in Section 3.2.2. Then, considering an alternative to Eq. (32) as:

$$\frac{\partial p_F(\mathbf{y})}{\partial y_q} = \sum_{i=1}^{n_\eta} \sum_{k=1}^{n_T} \left(\frac{1}{w_{i,k}} \frac{\partial p_{i,k}(\mathbf{y})}{\partial y_q} \right) w_{i,k}. \tag{40}$$

The expression in Eq. (40) involves a summation over a discrete random variable $w_{i,k}$ and an integration over a continuous random variable \mathbf{u} . This can be solved through simulation by generating samples of both random variables, as follows:

$$\frac{\partial p_F(\mathbf{y})}{\partial y_q} \approx \frac{\partial \bar{p}_F(\mathbf{y})}{\partial y_q} = \frac{1}{N} \sum_{j=1}^N \left(\frac{1}{w_{(i,k)^{(j)}}} \frac{\partial \bar{p}_{(i,k)^{(j)}}(\mathbf{y}, \mathbf{u}_{(i,k)^{(j)})})}{\partial y_q} \right), \tag{41}$$

where $\partial \bar{p}_F(\mathbf{y})/\partial y_q$ corresponds to an estimate of $\partial p_F(\mathbf{y})/\partial y_q$; N is the total number of samples; $(i, k)^{(j)}$, $j = 1, \dots, N$, are independent and identically distributed samples chosen from the set $I = \{1, \dots, n_\eta \times n_T\}$ with probability mass function $w_{i,k}$, where $i = 1, \dots, n_\eta$ and $k = 1, \dots, n_T$; the vector $\mathbf{u}_{(i,k)^{(j)}}$ is distributed according to $f_U^{IS,(i,k)}(\mathbf{u})$; and $\partial \bar{p}_{(i,k)^{(j)}}(\mathbf{y}, \mathbf{u}_{(i,k)^{(j)})})/\partial y_q$ is the estimate of the derivative of the effective contribution $\partial p_{(i,k)^{(j)}}(\mathbf{y}, \mathbf{u}_{(i,k)^{(j)})})/\partial y_q$ evaluated at the sample $\mathbf{u}_{(i,k)^{(j)}}$. To estimate the derivative of the effective contribution, it is necessary to estimate the term $\bar{\mu}_{i,k}(\mathbf{y})$ by evaluating the sampled direction $\mathbf{u}_{(i,k)^{(j)}}$ in Eq. (37), which means:

$$\begin{aligned} \frac{\partial \bar{p}_{(i,k)^{(j)}}(\mathbf{y}, \mathbf{u}_{(i,k)^{(j)})})}{\partial y_q} &\approx P[F_{i,k}] \mu_{i,k}(\mathbf{y}, \mathbf{u}_{(i,k)^{(j)})}) = \\ &P[F_{i,k}] \sum_{l=L}^{\infty} \frac{1}{l(1 - F_{R^2}(c_l(\mathbf{y}, \mathbf{u}_{(i,k)^{(j)})})^2)} \left(2c_{l+1}(\mathbf{y}, \mathbf{u}_{(i,k)^{(j)})}) \frac{\partial c_{l+1}(\mathbf{y}, \mathbf{u}_{(i,k)^{(j)})})}{\partial y_q} f_{R^2}(c_{l+1}(\mathbf{y}, \mathbf{u}_{(i,k)^{(j)})})^2) \right. \\ &\quad \left. - 2c_l(\mathbf{y}, \mathbf{u}_{(i,k)^{(j)})}) \frac{\partial c_l(\mathbf{y}, \mathbf{u}_{(i,k)^{(j)})})}{\partial y_q} f_{R^2}(c_l(\mathbf{y}, \mathbf{u}_{(i,k)^{(j)})})^2) \right). \end{aligned} \tag{42}$$

Eq. (41) yields the sensitivity of the first excursion probability estimator using the *Domain Decomposition Method*.

Finally, it can be easily proven that the coefficient of variation $\delta_{\partial p_F/\partial y_q}$ of the sensitivity estimator in Eq. (41) is equal to:

$$\delta_{\partial p_F/\partial y_q} = \frac{1}{\partial \bar{p}_F(\mathbf{y})/\partial y_q} \sqrt{\frac{1}{N(N-1)} \sum_{j=1}^N \left(\left(\frac{1}{w_{(i,k)^{(j)}}} \frac{\partial \bar{p}_{(i,k)^{(j)}}(\mathbf{y}, \mathbf{u}_{(i,k)^{(j)})}}{\partial y_q} \right) - \frac{\partial \bar{p}_F(\mathbf{y})}{\partial y_q} \right)^2}. \quad (43)$$

3.4. Practical implementation

The calculation of gradient estimates using Eq. (41) involves the partial derivatives $\partial c_{i,k}(\mathbf{y}, \mathbf{u})/\partial y_q$, with $q = 1, \dots, n_y$, for all the possible sampled directions. This can be done by directly differentiating Eq. (19) with respect to a design parameter y_q , resulting in:

$$\frac{\partial c_{i,k}(\mathbf{y}, \mathbf{u})}{\partial y_q} = -\frac{b_i}{(\mathbf{a}_{i,k}(\mathbf{y})^T \mathbf{u}) |\mathbf{a}_{i,k}(\mathbf{y})^T \mathbf{u}|} \left(\left(\frac{\partial \mathbf{a}_{i,k}(\mathbf{y})}{\partial y_q} \right)^T \mathbf{u} \right), \quad (44)$$

where $\partial \mathbf{a}_{i,k}(\mathbf{y})/\partial y_q$ denotes the derivative of vector $\mathbf{a}_{i,k}$ with respect to the design parameter y_q . As shown in Section 2.2, vector $\mathbf{a}_{i,k}(\mathbf{y})$ depends on the i th unit impulse response function $h_i(t, \mathbf{y})$, and its derivative can be calculated directly by differentiating Eq. (9) as follows:

$$\frac{\partial \mathbf{a}_{i,k}(\mathbf{y})}{\partial y_q} = \sum_{m=1}^k \Delta t \epsilon_m \frac{\partial h_i(t_k - t_m, \mathbf{y})}{\partial y_q} \boldsymbol{\psi}_m, \quad (45)$$

where $\partial h_i(t, \mathbf{y})/\partial y_q$ is the partial derivative of the i th unit impulse response function with respect to the design parameter y_q . From Eq. (7) it is clear that the unit impulse response function depends on the mass matrix, damping matrix, coupling vector and spectral properties (that is, eigenvectors and eigenvalues). Therefore, the calculation of the partial derivative of the unit impulse response function with respect to a design parameter, can be achieved by applying the chain rule for differentiation, as detailed in Appendix C. It is worth noting that the partial derivative of the eigenvectors and eigenvalues can be obtained using the method proposed in [34].

The numerical implementation for calculating the reliability and sensitivity estimates can be achieved using Eqs. (29) and (40), which require one dynamic analysis and one sensitivity analysis, respectively. Both equations can be evaluated with the same samples, as the weights $w_{i,k}$ and $f^{IS,(i,k)}$ use identical indices in both cases. Consequently, the sensitivity analysis becomes a byproduct of the reliability analysis.

3.5. Summary

The application of the Domain Decomposition Method for calculating the gradient of the first excursion probability with respect to a design parameter, in the context of a linear system subjected to Gaussian loading, can be achieved by following these steps:

1. Define the basic information of the structural model. This includes the matrices \mathbf{M} , \mathbf{C} , and \mathbf{K} , the vector representing the structural properties of the system, \mathbf{y} , and the threshold vector \mathbf{b} .
2. Define the Gaussian load using the Karhunen–Loève expansion following Eq. (1).
3. Calculate the vector that characterizes the responses $\mathbf{a}_{i,k}$ with $i = 1, \dots, n_\eta$ and $k = 1, \dots, n_T$ using Eq. (9), and calculate the vector $\partial \mathbf{a}_{i,k}(\mathbf{y})/\partial y_q$ with $i = 1, \dots, n_\eta$ and $k = 1, \dots, n_T$ using Eq. (45) and Appendix C.
4. Calculate the design points $\mathbf{z}_{i,k}^*(\mathbf{y})$, reliability indices $\beta_{i,k}(\mathbf{y})$ and weights $w_{i,k}$ using Eqs. (13), (14) and (B.7), respectively.
5. Sample (with replacement) a total of N pair of indices $(i, k)^{(j)}$, $j = 1, \dots, N$, from the set $I = \{1, \dots, n_\eta \times n_T\}$ with probability $w_{i,k}$. Then, generate samples $\mathbf{u}_{(i,k)^{(j)}}$ following the procedure described in Appendix B.
6. For each sample, calculate and sort the distances $c_{i,k}(\mathbf{y}, \mathbf{u}_{(i,k)^{(j)})}$ with $i = 1, \dots, n_\eta$ and $k = 1, \dots, n_T$ in ascending order of magnitude using Eqs. (19) and (20). Then, implement the sorted notation detailed in Section 3.2.2 and identify the index L associated to each sample.
7. For each sample, calculate the derivative of the distances $\partial c_{i,k}(\mathbf{y}, \mathbf{u}_{(i,k)^{(j)})}/\partial y_q$ with $i = 1, \dots, n_\eta$ and $k = 1, \dots, n_T$ using Eq. (44), and the sort the values in the same order as in the previous step.
8. Calculate the first excursion probability using Eq. (29) and its coefficient of variation using Eq. (31).
9. Calculate the sensitivity estimate using Eq. (41) and its coefficient of variation using Eq. (43).

4. Examples

This section presents two examples that demonstrate the application of the proposed framework. The first example comprises a two-degree-of-freedom representation of a quarter-car model that considers nonproportional damping. The second example involves a large-scale finite element model of a curved bridge, demonstrating that the method is also applicable in cases with proportional damping. The results are compared with a reference method to assess the efficiency of this approach.

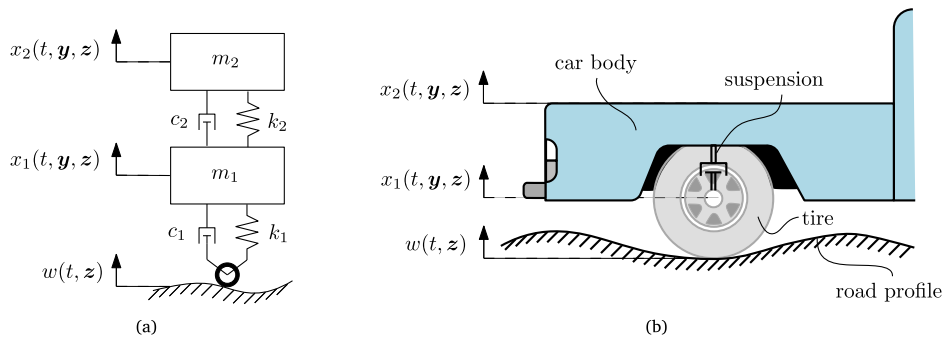


Fig. 5. Example 1: Quarter-car model. (a) 2-degree-of-freedom representation. (b) Physical representation.

4.1. Example 1: Quarter-car model

The first example is a quarter-car model, which consist in a two-degree-of-freedom idealization of the suspension of a car, as shown in Fig. 5. This model is based on an example presented in [49]. The dynamics of the problem is governed by the following two ordinary differential equations:

$$\begin{bmatrix} m_1 & 0 \\ 0 & m_2 \end{bmatrix} \begin{Bmatrix} \ddot{x}_1(t, y, z) \\ \ddot{x}_2(t, y, z) \end{Bmatrix} + \begin{bmatrix} c_1 + c_2 & -c_2 \\ -c_2 & c_2 \end{bmatrix} \begin{Bmatrix} \dot{x}_1(t, y, z) \\ \dot{x}_2(t, y, z) \end{Bmatrix} + \begin{bmatrix} k_1 + k_2 & -k_2 \\ -k_2 & k_2 \end{bmatrix} \begin{Bmatrix} x_1(t, y, z) \\ x_2(t, y, z) \end{Bmatrix} = \begin{Bmatrix} k_1 w(t, z) + c_1 \dot{w}(t, z) \\ 0 \end{Bmatrix}, \quad (46)$$

where $m_1 = 15$ kg and $m_2 = 290$ kg represent the unsprung and sprung masses of a quarter of the car, respectively. The tire stiffness is $k_1 = 191\,000$ N/m, while the suspension stiffness is $k_2 = 16\,200$ N/m. Additionally, the damping coefficients for the tire and suspension are $c_1 = 100$ Ns/m and $c_2 = 2500$ Ns/m, respectively.

The load acting on the quarter-car model is the road profile $w(t, z)$, which is modeled as a zero-mean Gaussian random field with a squared exponential covariance kernel, with a correlation length $L = 3$ m and a standard deviation of 0.01 m. The car speed considered is 25 m/s over a distance of 125 m. The dimension along the road is discretized into 1001 equidistant points, considering a total of $n_{KL} = 1001$ terms. The time is discretized in intervals of $\Delta t = 0.005$ s, which means that the problem dynamics have a total duration of 5 s. It is also assumed that the car starts from a rest position in the x_1 and x_2 coordinates.

In order to assess the comfort of a car while driving over a road profile, it is common to control two responses of interest: the acceleration of the sprung mass and the suspension stroke (the relative displacement between the car body and the unsprung mass), with the latter being considered in this example. Specifically, the response of interest is the displacement of mass m_2 with respect to mass m_1 , expressed as $\eta(t, y, z) = |x_2(t, y, z) - x_1(t, y, z)|$, which involves a total of $n_\eta = 1001$ elementary failure domains. The threshold level is set at $b = 3.5 \times 10^{-2}$ m, and the first excursion probability is estimated using the Domain Decomposition Method, resulting in $\hat{p}_F = 5.1 \times 10^{-3}$.

The objective is to estimate the sensitivity of the first excursion probability with respect to the mass m_2 and the stiffness k_2 of the model, that is with respect to the design vector $\mathbf{y} = [m_2, k_2]^T$, using both the Domain Decomposition Method and Directional Sampling. In the latter approach, the estimation focuses on the effective contributions by directly sampling unit directions according to Eq. (22), without introducing the importance sampling density.

The evolution of the sensitivity estimates and their coefficient of variation with respect to the number of samples is shown in Figs. 6 and 7. In this example, a total of 10^6 samples are considered. The sensitivity estimates converge to similar values for both methods. The Domain Decomposition Method provides a more stable estimator compared to Directional Sampling, with a significantly lower coefficient of variation in all the estimates. Considering an acceptable stabilization point for the estimates when they reach a 20% coefficient of variation, it can be observed that the Domain Decomposition Method requires approximately 400 samples, while Directional Sampling requires around 10^6 samples. In addition, the results have been validated using finite differences, where the sensitivity estimator has been estimated with 2×10^6 samples (1×10^6 samples in each of the forward and backward steps). The comparison with finite differences, in which the proposed technique achieves a 5% coefficient of variation, is presented in Table 3. There is an excellent match between the sensitivity estimates calculated with DDM and finite differences.

The sensitivity analysis with respect to the design parameters m_2 and k_2 is particularly relevant for assessing the comfort of the car. As shown in Fig. 6, for the chosen parameters, an increase in the vehicle's body mass results in a higher failure probability. This is due to a potential decrease in the system's natural frequency, which makes the system more sensitive to low-frequency perturbations in the road profile, ultimately leading to an increased response of interest. Furthermore, as shown in Fig. 7, an increase in the stiffness k_2 also leads to a higher failure probability. The reason for this is that a stiffer suspension makes the vehicle more reactive to road irregularities, thereby increasing the system's failure probability.

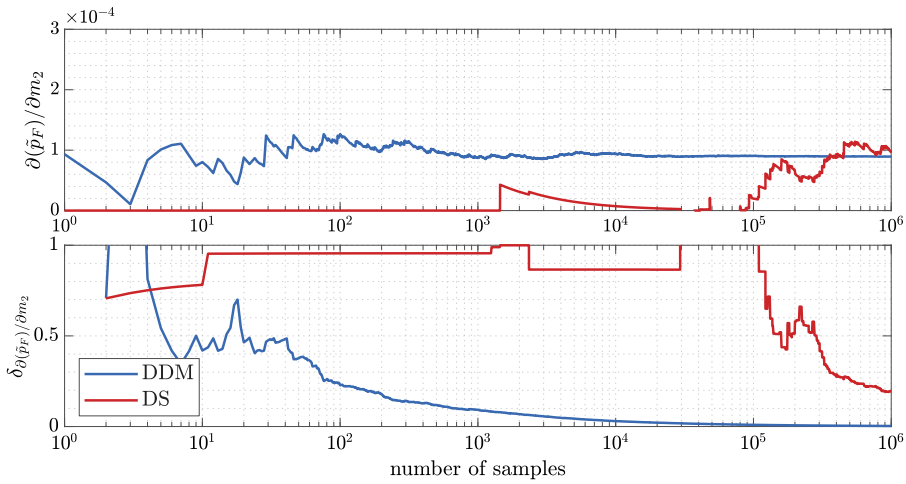


Fig. 6. Example 1: Evolution of the sensitivity estimator (upper figure) and its coefficient of variation (lower figure) associated with m_2 with respect to the number of samples, using both the Domain Decomposition Method (DDM) and Directional Sampling (DS).

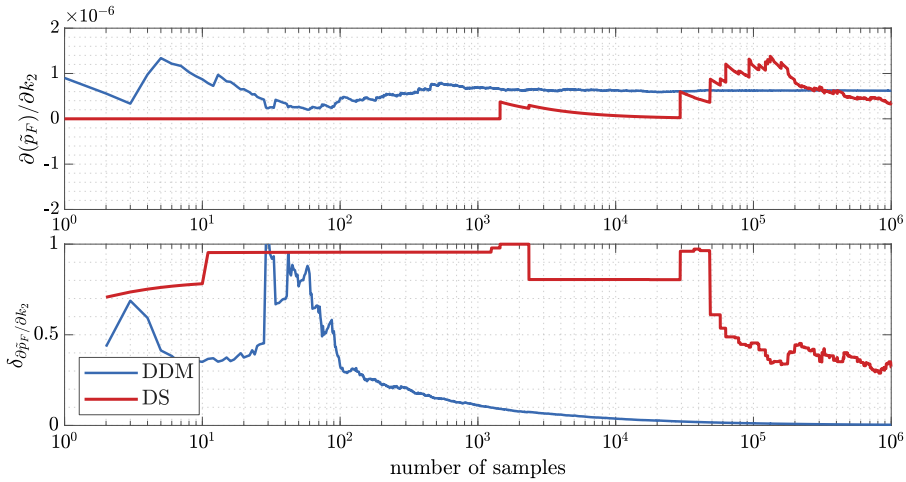


Fig. 7. Example 1: Evolution of the sensitivity estimator (upper figure) and its coefficient of variation (lower figure) associated with k_2 with respect to the number of samples, using both the Domain Decomposition Method (DDM) and Directional Sampling (DS).

Table 3
Comparison of sensitivity estimates obtained using the Domain Decomposition method (DDM) achieving a 5% coefficient of variation, against reference results from finite differences (FD).

	DDM	FD
$\frac{\partial \bar{p}_F}{\partial m_2}$	8.90×10^{-5}	8.96×10^{-5}
$\frac{\partial \bar{p}_F}{\partial k_2}$	6.33×10^{-7}	6.25×10^{-7}

4.2. Example 2: Curved bridge subject to Gaussian ground excitation

The second example corresponds to a three-dimensional finite element model of a curved bridge, which comprises 10068 degrees of freedom, illustrated in Figs. 8 and 9. This model is based on an example presented in [7]. The superstructure of the bridge is modeled as a monolithic box girder composed of shell and beam elements. It is curved in the plane x - y with a total length of 119 m constituted of five spans with length of 24 m, 20 m, 23 m, 25 m, and 27 m, respectively. The substructure is modeled with four

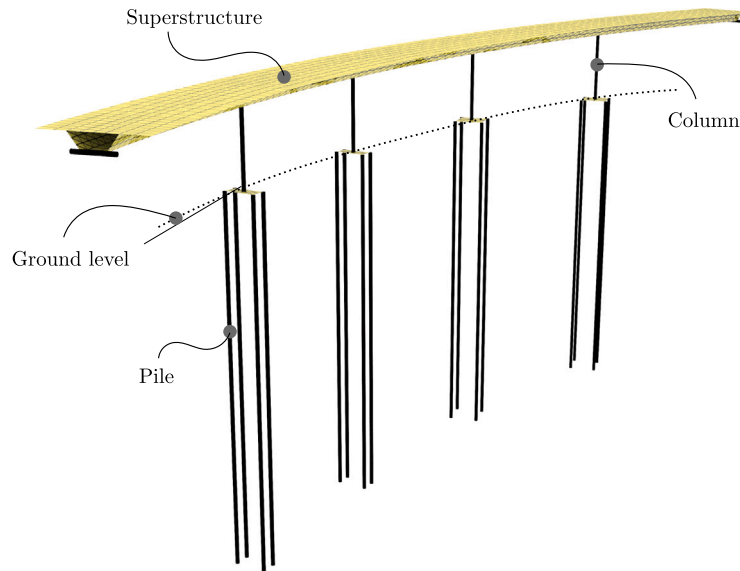


Fig. 8. Example 2: Perspective view of the finite element model of the curved bridge.

columns, each supported by four piles, using beam and shell elements. The columns, labeled as C_k , for $k = 1, 2, 3, 4$, have circular cross section with a diameter of 1.6 m and a height of 8 m, while the piles have a diameter of 0.6 m and a height of 35 m. The interaction between the piles and the soil is modeled using linear springs with translational stiffness in the x and y directions, varying linearly from 112 MN/m at the deepest point of the pile to 0 MN/m at the ground level. All elements of the model have the same material properties, which correspond to reinforced concrete, with a Young's modulus of $E = 2.09 \times 10^{10}$ N/m², a Poisson's ratio $\nu = 0.2$, and a density $\rho = 2500$ kg/m³. The classical damping considered is equal to 3% for all mode shapes.

The stochastic ground acceleration acting on the bridge is modeled as a discrete white noise process with a spectral density of $S = 5 \times 10^4$ m²/s³, over a total duration of $T = 10$ s, discretized into 1001 time instants of duration $\Delta t = 0.01$ s. It is applied at an angle of 45 degrees with respect to the x axis. Additionally, the discrete white noise process passes through a Clough–Penzien filter [50] and is modulated by the following function $m(t)$:

$$m(t) = \begin{cases} (t/5)^2 & 0 \leq t \leq 5 \text{ [s]} \\ 1 & 5 < t \leq 6 \text{ [s]} \\ e^{-(t-6)^2} & t > 6 \text{ [s]} \end{cases} \quad (47)$$

The Karhunen–Loève representation for the ground acceleration considers a total of $n_{KL} = 1001$ terms. It is also assumed that the structure starts from a rest position.

The responses of interest are defined as the drift of the columns in either x or y direction. The failure event corresponds to each of the responses of interest exceeding a threshold of $b = 0.02$ m. That means, eight responses of interest that can be evaluated at every time instant, resulting in a total of 8008 elementary failure domains. The response has been calculated with a truncation of 100 mode shapes for the dynamic analysis. The first excursion probability is calculated using the Domain Decomposition Method resulting in $\bar{p}_F \approx 3.0 \times 10^{-3}$.

The objective is to estimate the sensitivity of the first excursion probability within the framework of the Domain Decomposition Method. The sensitivity is estimated with respect to the design vector $\mathbf{y} = [y_1, y_2, y_3, y_4]^T$, where y_j denotes the diameter of the j th column C_j , as illustrated in Fig. 9.

The sensitivity of the first excursion probability is estimated using both the Domain Decomposition Method and Directional Sampling with respect to the design parameter y_1 . In the latter approach, the same considerations discussed in Section 4.1 are followed. The evolution of the sensitivity estimator and its coefficient of variation is shown in Fig. 10, where a total of 10^6 samples is considered. The sensitivity estimates converge to a similar value for both methods. The Domain Decomposition Method provides a more stable estimator compared to Directional Sampling. This can be confirmed by observing the lower plot in Fig. 10, where the Domain Decomposition Method has a coefficient of variation that is considerably lower than that of Directional Sampling. Considering an acceptable stabilization point for the estimator when it reaches a 20% coefficient of variation, it can be observed that the Domain Decomposition Method requires approximately 2000 samples, while Directional Sampling cannot reach this value with the samples used.

The evolution of the sensitivity estimates with respect to the design parameters y_q , where $q = 1, 2, 3, 4$, and the evolution of their coefficient of variation, are shown in Fig. 11. The results indicate that increasing the diameter of columns 1 and 2 leads to an increase in the failure probability of the system, with both columns having almost the same influence, as seen in the superimposed

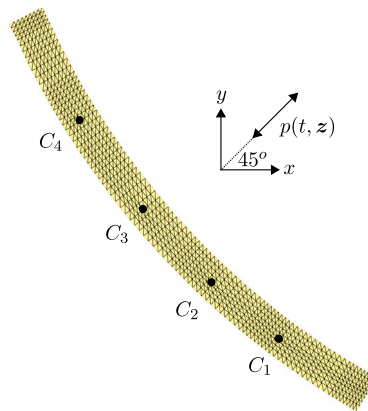


Fig. 9. Example 2: Top view of the finite element model of the curved bridge.

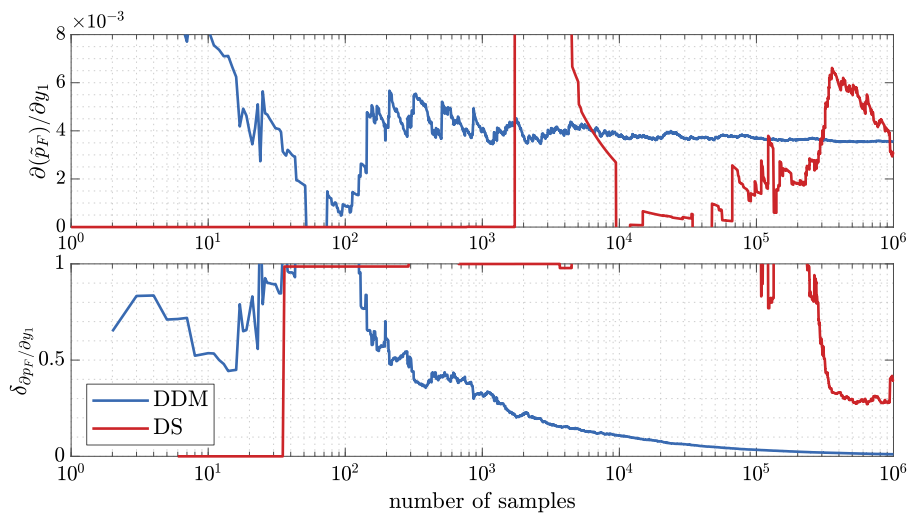


Fig. 10. Example 2: Evolution of the sensitivity estimator (upper figure) and its coefficient of variation (lower figure) associated with y_1 with respect to the number of samples, using both the Domain Decomposition Method (DDM) and Directional Sampling (DS).

results of the curves associated with y_1 and y_2 . In contrast, increasing the diameter of columns 3 and 4 (primarily) results in a decrease in the failure probability of the system. Considering the same criterion as before, the sensitivity estimates with respect to y_1 and y_2 stabilize with approximate 2000 samples. In the case of the sensitivity estimator with respect to y_3 , stabilizes with approximately 4500 samples, while the sensitivity estimator with respect to y_4 , stabilizes with approximately 1000 samples.

To understand the physical meaning of the presented results, Fig. 12 illustrates a schematic associated with the most predominant failure response: the displacement of column C_4 exceeding the prescribed threshold in the x direction. According to the results of the sensitivity estimates presented in Fig. 11, an increase in the diameter of columns C_1 and C_2 causes the bridge (viewed in plan) to tend to rotate around a point between these columns. This results in increased displacements in columns C_3 and C_4 , consequently increasing the system's failure probability. Conversely, an increase in the diameter of columns C_3 and C_4 helps to control the total translation of the bridge, which leads to a reduction in the failure probability of the system.

5. Conclusions and outlook

This contribution has explored the application of the Domain Decomposition Method for estimating the sensitivity of the first excursion probability of a linear system with nonproportional damping subject to a Gaussian loading. The sensitivity is calculated as the partial derivative of the first excursion probability with respect to design parameters that influence the structural response. These derivatives involve the sensitivity analysis of the unit impulse response functions, as well as the spectral properties of the system, including the eigenvectors and eigenvalues.

The proposed framework collects valuable information of the failure domain by exploring it in a directional way. For each line explored, the information of the effective contribution of the failure probability and its gradient for each elementary failure domain

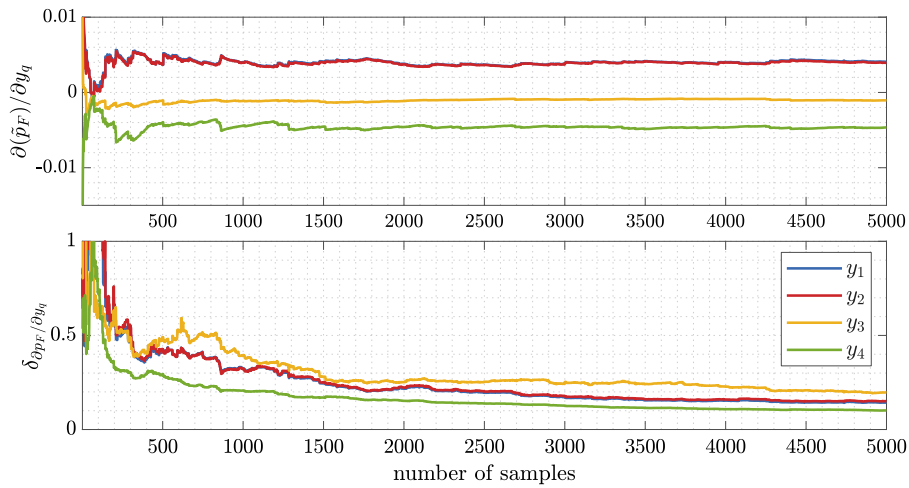


Fig. 11. Example 2: Evolution of the sensitivity estimator (upper figure) and its coefficient of variation (lower figure) associated with y_q ($q = 1, 2, 3, 4$) with respect to the number of samples, using the Domain Decomposition Method (DDM).

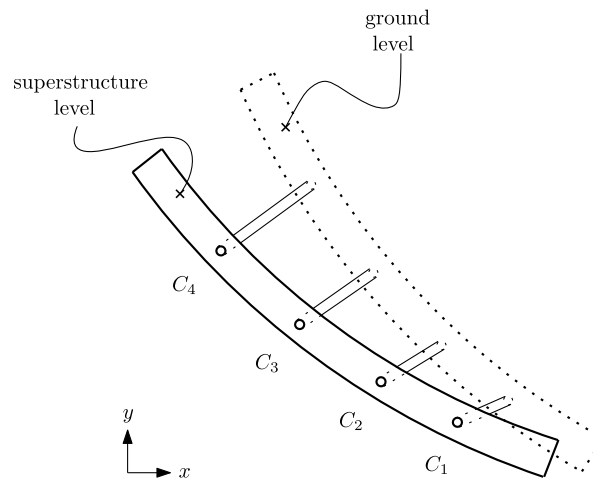


Fig. 12. Example 2: Schematic representation of a predominant failure response.

is incorporated into both estimators. For this reason, the calculation of the sought sensitivities is achieved with a reduced number of samples, demonstrating high efficiency and stability. Furthermore, the sensitivities are estimated as a byproduct of the reliability analysis.

Future extensions of the presented research could explore the following:

- The design of a modified importance sampling density function, which could improve the efficiency of the sensitivity estimates.
- The effect of the weights on the estimation of effective contributions.
- The calculation of sensitivity estimates with respect to excitation parameters, such as the frequencies of the Clough–Penzien model filters.
- The application of the proposed method in the context of reliability-based design optimization (RBO) problems.

The above-mentioned issues are currently being investigated by the authors.

CRedit authorship contribution statement

Mauricio A. Misraji: Writing – original draft, Visualization, Validation, Software, Resources, Methodology, Investigation, Formal analysis, Conceptualization. **Marcos A. Valdebenito:** Writing – review & editing, Validation, Supervision, Methodology, Conceptualization. **Matthias G.R. Faes:** Writing – review & editing, Supervision, Project administration, Methodology, Funding acquisition, Conceptualization.

Declaration of competing interest

The authors declare that they have no known competing financial interests or personal relationships that could have appeared to influence the work reported in this paper.

Appendix A. Gradient of the failure probability

The deduction of the expression presented in Eq. (12) can be done by writing the first excursion probability presented in Eq. (11) as:

$$p_F(\mathbf{y}) = \int_{\mathbf{z} \in \mathbb{R}^{KL}} H(-g(\mathbf{y}, \mathbf{z})) f_Z(\mathbf{z}) d\mathbf{z}, \quad (\text{A.1})$$

where $H(\cdot)$ denotes the step function. Then, the differentiation of Eq. (A.1) with respect to a design parameter y_q , leads to:

$$\frac{\partial p_F(\mathbf{y})}{\partial y_q} = - \int_{\mathbf{z} \in \mathbb{R}^{KL}} \delta(-g(\mathbf{y}, \mathbf{z})) \frac{\partial g(\mathbf{y}, \mathbf{z})}{\partial y_q} f_Z(\mathbf{z}) d\mathbf{z}, \quad q = 1, \dots, n_y, \quad (\text{A.2})$$

where $\delta(\cdot)$ corresponds to Dirac delta. Furthermore, using the following identity [51]:

$$\int_{\mathbb{R}^n} f_1(\mathbf{x}) \delta(f_2(\mathbf{x})) d\mathbf{x} = \int_{f_2(\mathbf{x})=0} \frac{f_1(\mathbf{x})}{\|\nabla f_2(\mathbf{x})\|} d\sigma, \quad (\text{A.3})$$

being σ a differential surface element, $f_1(\mathbf{x})$ a function, and $f_2(\mathbf{x})$ a differentiable function, with a non-zero gradient at the points where $f_2(\mathbf{x}) = 0$. Then, using the identity of Eq. (A.3) in Eq. (A.1), the expression for the gradient of the failure probability becomes [52]:

$$\frac{\partial p_F(\mathbf{y})}{\partial y_q} = - \int_{g(\mathbf{y}, \mathbf{z})=0} \frac{\partial g(\mathbf{y}, \mathbf{z})}{\partial y_q} \frac{1}{\|\nabla_{\mathbf{z}} g(\mathbf{y}, \mathbf{z})\|} f_Z(\mathbf{z}) dS, \quad q = 1, \dots, n_y. \quad (\text{A.4})$$

Appendix B. Importance sampling density $f_U^{\text{IS},(i,k)}(\mathbf{u})$ and samples generation

The importance sampling density function $f_U^{\text{IS},(i,k)}(\mathbf{u})$ is constructed based on the ideas proposed in [5,7,45], with the difference that each effective contribution $p_{i,k}$ has its own importance sampling density function, defined as:

$$f_U^{\text{IS},(i,k)}(\mathbf{u}) = f_U(\mathbf{u}|F_{i,k}), \quad (\text{B.1})$$

where $f_U(\mathbf{u}|F_{i,k})$ is the probability density associated with the direction \mathbf{u} on the occurrence of an elementary failure event $F_{i,k}$, which can be analyzed by applying Bayes' theorem, as follows:

$$f_U(\mathbf{u}|F_{i,k}) = \frac{P[\mathbf{u} \cap F_{i,k}]}{P[F_{i,k}]} \quad (\text{B.2})$$

$$= \frac{f_U(\mathbf{u}) P[\mathbf{u}|F_{i,k}]}{P[F_{i,k}]} \quad (\text{B.3})$$

$$= \frac{f_U(\mathbf{u}) P[\mathbf{u}|F_{i,k}]}{2\Phi_{\mathbf{Z}}(-\beta_{i,k})}, \quad (\text{B.4})$$

where $P[\mathbf{u}|F_{i,k}]$ is the probability of occurrence of the elementary failure event $F_{i,k}$ given a particular direction \mathbf{u} in the standard Gaussian space. This term can be expressed as:

$$P[\mathbf{u}|F_{i,k}] = 1 - F_{R^2}(c_{i,k}(\mathbf{y}, \mathbf{u})^2), \quad (\text{B.5})$$

and the proposed importance sampling density function becomes:

$$f_U^{\text{IS},(i,k)}(\mathbf{u}) = \frac{f_U(\mathbf{u}) (1 - F_{R^2}(c_{i,k}(\mathbf{y}, \mathbf{u})^2))}{2\Phi_{\mathbf{Z}}(-\beta_{i,k})}. \quad (\text{B.6})$$

The process of generating samples $\mathbf{u}^{(j)}$, $j = 1, \dots, N$ following $f_U^{\text{IS},(i,k)}(\mathbf{u})$ is done by the following procedure [5–7]:

1. Set $j = 1$.
2. Draw a pair of indices (I, K) from the set $\Omega = \{(i, k) : i \in \{1, \dots, n_\eta\}, k \in \{1, \dots, n_T\}\}$ with probability proportional to the weights $w_{i,k}$, $i = 1, \dots, n_\eta$, $k = 1, \dots, n_T$, defined as follows:

$$w_{i,k} = \frac{P[F_{i,k}]}{\sum_{h=1}^{n_\eta} \sum_{j=1}^{n_T} P[F_{h,j}]}. \quad (\text{B.7})$$

3. Generate a sample \mathbf{z} of the random vector \mathbf{Z} , together with the realizations of u_1 and u_2 , which follow a uniform distribution between 0 and 1.

4. Calculate $\alpha = -\Phi^{-1}((1 - u_1)\Phi(-\beta_{i,k}))$, where $\Phi^{-1}(\cdot)$ denotes the inverse cumulative standard Gaussian distribution.
5. Calculate $\mathbf{a}_{I,K}^*(\mathbf{y}) = \mathbf{a}_{I,K}(\mathbf{y}) / \|\mathbf{a}_{I,K}(\mathbf{y})\|$, where $\mathbf{a}_{I,K}(\mathbf{y})$ is defined in Eq. (9).
6. Define \mathbf{z}^* as:

$$\mathbf{z}^* = \begin{cases} \mathbf{z} + (\alpha - \mathbf{z}^T \mathbf{a}_{I,K}^*(\mathbf{y})) \mathbf{a}_{I,K}^*(\mathbf{y}) & \text{if } u_2 \leq 1/2 \\ -\mathbf{z} - (\alpha - \mathbf{z}^T \mathbf{a}_{I,K}^*(\mathbf{y})) \mathbf{a}_{I,K}^*(\mathbf{y}) & \text{otherwise} \end{cases}, \quad (\text{B.8})$$

and calculate the desired sample as $\mathbf{u}^{(j)} = \mathbf{z}^* / \|\mathbf{z}^*\|$.

7. If $j = N$, stop the procedure; otherwise, increment j by 1 and return to step 2.

Appendix C. Derivative of unit impulse response function

Eq. (7) can be recast as:

$$h_i(t, \mathbf{y}) = \sum_{r=1}^{2n_D} A_{r,i}(\mathbf{y}) B_r(t, \mathbf{y}), \quad (\text{C.1})$$

where $i = 1, \dots, n_\eta$. Then, the terms $A_{r,i}(\mathbf{y})$ and $B_r(t, \mathbf{y})$ are defined as:

$$A_{r,i}(\mathbf{y}) = \frac{\gamma_i^T \boldsymbol{\phi}_r(\mathbf{y}) \boldsymbol{\phi}_r(\mathbf{y})^T \mathbf{g}_a(\mathbf{y})}{\boldsymbol{\phi}_r(\mathbf{y})^T \mathbf{M}_a(\mathbf{y}) \boldsymbol{\phi}_r(\mathbf{y})}, \quad (\text{C.2})$$

$$B_r(t, \mathbf{y}) = e^{\lambda_r(\mathbf{y})t}, \quad (\text{C.3})$$

where $r = 1, \dots, 2n_D$ and $i = 1, \dots, n_\eta$. Therefore, the partial derivative of the unit impulse response function in Eq. (C.1) with respect to the design parameter y_q , where $q = 1, \dots, n_Y$, is given by:

$$\frac{\partial h_i(t, \mathbf{y})}{\partial y_q} = \sum_{r=1}^{2n_D} \left(\frac{\partial A_{r,i}(\mathbf{y})}{\partial y_q} B_r(t, \mathbf{y}) + A_{r,i}(\mathbf{y}) \frac{\partial B_r(t, \mathbf{y})}{\partial y_q} \right). \quad (\text{C.4})$$

Then, considering $A_{r,i}^{(1)}(\mathbf{y}) = \gamma_i^T \boldsymbol{\phi}_r(\mathbf{y}) \boldsymbol{\phi}_r(\mathbf{y})^T \mathbf{g}_a(\mathbf{y})$ and $A_r^{(2)}(\mathbf{y}) = \boldsymbol{\phi}_r(\mathbf{y})^T \mathbf{M}_a(\mathbf{y}) \boldsymbol{\phi}_r(\mathbf{y})$, it is possible to calculate the derivative of Eq. (C.4) as:

$$\frac{\partial A_{r,i}(\mathbf{y})}{\partial y_q} = \left(\frac{\partial A_{r,i}^{(1)}(\mathbf{y})}{\partial y_q} A_r^{(2)}(\mathbf{y}) - A_{r,i}^{(1)}(\mathbf{y}) \frac{\partial A_r^{(2)}(\mathbf{y})}{\partial y_q} \right) \frac{1}{(A_r^{(2)})^2} \quad (\text{C.5})$$

$$\frac{\partial B_r(t, \mathbf{y})}{\partial y_q} = t e^{\lambda_r t} \frac{\partial \lambda_r}{\partial y_q}. \quad (\text{C.6})$$

where

$$\frac{\partial A_{r,i}^{(1)}(\mathbf{y})}{\partial y_q} = \gamma_i^T \left(\frac{\partial \boldsymbol{\phi}_r(\mathbf{y})}{\partial y_q} \boldsymbol{\phi}_r(\mathbf{y})^T \mathbf{g}_a(\mathbf{y}) + \boldsymbol{\phi}_r(\mathbf{y}) \left(\frac{\partial \boldsymbol{\phi}_r(\mathbf{y})^T}{\partial y_q} \mathbf{g}_a(\mathbf{y}) + \boldsymbol{\phi}_r(\mathbf{y})^T \frac{\partial \mathbf{g}_a(\mathbf{y})}{\partial y_q} \right) \right) \quad (\text{C.7})$$

$$\frac{\partial A_r^{(2)}(\mathbf{y})}{\partial y_q} = \frac{\partial \boldsymbol{\phi}_r(\mathbf{y})^T}{\partial y_q} \mathbf{M}_a(\mathbf{y}) \boldsymbol{\phi}_r(\mathbf{y}) + \boldsymbol{\phi}_r(\mathbf{y})^T \left(\frac{\partial \mathbf{M}_a(\mathbf{y})}{\partial y_q} \boldsymbol{\phi}_r(\mathbf{y}) + \mathbf{M}_a(\mathbf{y}) \frac{\partial \boldsymbol{\phi}_r(\mathbf{y})}{\partial y_q} \right). \quad (\text{C.8})$$

It is worth noting that, to implement Eq. (C.4), it is necessary to calculate the partial derivatives of the eigenvalue $\partial \lambda_r(\mathbf{y}) / \partial y_q$ and the eigenvector $\partial \boldsymbol{\phi}_r(\mathbf{y}) / \partial y_q$. This can be done by following the approach proposed in [34]. The advantage of this framework is that the calculation of derivatives for the r th eigenvalue and eigenvector does not depend on other eigenvalues and eigenvectors [53]. This is particularly important when simplifying the analysis by neglecting the total number of mode shapes needed to calculate the responses of interest. Therefore, the sought derivatives can be calculated solving the following system of equations:

$$\begin{pmatrix} \mathbf{K}_a(\mathbf{y}) - \lambda_r(\mathbf{y}) \mathbf{M}_a(\mathbf{y}) & -\mathbf{M}_a(\mathbf{y}) \boldsymbol{\phi}_r(\mathbf{y}) \\ -\boldsymbol{\phi}_r(\mathbf{y})^T \mathbf{M}_a(\mathbf{y}) & 0 \end{pmatrix} \begin{pmatrix} \frac{\partial \boldsymbol{\phi}_r(\mathbf{y})}{\partial y_q} \\ \frac{\partial \lambda_r(\mathbf{y})}{\partial y_q} \end{pmatrix} = \begin{pmatrix} - \left(\frac{\partial \mathbf{K}_a(\mathbf{y})}{\partial y_q} - \lambda_r(\mathbf{y}) \frac{\partial \mathbf{M}_a(\mathbf{y})}{\partial y_q} \right) \boldsymbol{\phi}_r(\mathbf{y}) \\ \frac{1}{2} \boldsymbol{\phi}_r(\mathbf{y})^T \frac{\partial \mathbf{M}_a(\mathbf{y})}{\partial y_q} \boldsymbol{\phi}_r(\mathbf{y}) \end{pmatrix}. \quad (\text{C.9})$$

It is important noting that Eq. (C.9) is calculated under the assumption that the mode shapes are normalized, such as $\boldsymbol{\phi}_r(\mathbf{y})^T (-\mathbf{M}_a(\mathbf{y})) \boldsymbol{\phi}_r(\mathbf{y}) = 1$, and applies for the case without repeated eigenvalues.

Data availability

Data will be made available on request.

References

- [1] T. Soong, M. Grigoriu, *Random Vibration of Mechanical and Structural Systems*, Prentice Hall, Englewood Cliffs, New Jersey, 1993.
- [2] D. García, M. Rosales, R. Sampaio, Dynamic behaviour of a timber footbridge with uncertain material properties under a single deterministic walking load, *Struct. Saf.* 77 (2019) 10–17, <http://dx.doi.org/10.1016/j.strusafe.2018.11.001>, URL <http://www.sciencedirect.com/science/article/pii/S0167473018301127>.
- [3] D. Honfi, A. Mårtensson, S. Thelandersson, Reliability of beams according to eurocodes in serviceability limit state, *Eng. Struct.* 35 (2012) 48–54, <http://dx.doi.org/10.1016/j.engstruct.2011.11.003>.
- [4] M. Huang, C. Chan, W. Lou, Optimal performance-based design of wind sensitive tall buildings considering uncertainties, *Comput. Struct.* 98–99 (2012) 7–16, <http://dx.doi.org/10.1016/j.compstruc.2012.01.012>.
- [5] S. Au, J. Beck, First excursion probabilities for linear systems by very efficient importance sampling, *Probabilistic Eng. Mech.* 16 (3) (2001) 193–207.
- [6] L. Katafygiotis, S. Cheung, Domain decomposition method for calculating the failure probability of linear dynamic systems subjected to Gaussian Stochastic loads, *J. Eng. Mech.* 132 (5) (2006) 475–486.
- [7] M. Misraji, M. Valdebenito, H. Jensen, C. Mayorga, Application of directional importance sampling for estimation of first excursion probabilities of linear structural systems subject to stochastic Gaussian loading, *Mech. Syst. Signal Process.* 139 (2020) 106621, <http://dx.doi.org/10.1016/j.ymsp.2020.106621>, URL <http://www.sciencedirect.com/science/article/pii/S0888327020300078>.
- [8] M. Valdebenito, P. Wei, J. Song, M. Beer, M. Broggi, Failure probability estimation of a class of series systems by multidomain line sampling, *Reliab. Eng. Syst. Saf.* 213 (2021) 107673, <http://dx.doi.org/10.1016/j.res.2021.107673>, URL <https://www.sciencedirect.com/science/article/pii/S0951832021002118>.
- [9] S. Adhikari, *Structural dynamic analysis with generalized damping models*, Mechanical engineering and solid mechanics series, ISTE ;, London ;, 2014, Includes bibliographical references and index. - Description based on print version record.
- [10] M. Valdebenito, H. Jensen, G. Schuëller, F. Caro, Reliability sensitivity estimation of linear systems under stochastic excitation, *Comput. Struct.* 92–93 (2012) 257–268, <http://dx.doi.org/10.1016/j.compstruc.2011.10.020>.
- [11] M. Valdebenito, M. Misraji, H. Jensen, C. Mayorga, Sensitivity estimation of first excursion probabilities of linear structures subject to stochastic Gaussian loading, *Comput. Struct.* 248 (2021) 106482, <http://dx.doi.org/10.1016/j.compstruc.2021.106482>, URL <https://www.sciencedirect.com/science/article/pii/S0045794921000043>.
- [12] S. Benfratello, S. Caddemi, G. Muscolino, Gaussian and non-Gaussian stochastic sensitivity analysis of discrete structural system, *Comput. Struct.* 78 (1) (2000) 425–434, [http://dx.doi.org/10.1016/S0045-7949\(00\)00086-9](http://dx.doi.org/10.1016/S0045-7949(00)00086-9), URL <http://www.sciencedirect.com/science/article/pii/S0045794900000869>.
- [13] J. Chen, Z. Wan, M. Beer, A global sensitivity index based on fréchet derivative and its efficient numerical analysis, *Probabilistic Eng. Mech.* 62 (2020) 103096, <http://dx.doi.org/10.1016/j.probenmech.2020.103096>, URL <http://www.sciencedirect.com/science/article/pii/S0266892020300837>.
- [14] T. Hien, M. Kleiber, Stochastic design sensitivity in structural dynamics, *Internat. J. Numer. Methods Engrg.* 32 (6) (1991) 1247–1265, <http://dx.doi.org/10.1002/nme.1620320606>, arXiv:<https://onlinelibrary.wiley.com/doi/pdf/10.1002/nme.1620320606>, URL <https://onlinelibrary.wiley.com/doi/abs/10.1002/nme.1620320606>.
- [15] G. Muscolino, R. Santoro, A. Sofi, Explicit reliability sensitivities of linear structures with interval uncertainties under stationary stochastic excitation, *Struct. Saf.* 52, Part B (2015) 219–232, <http://dx.doi.org/10.1016/j.strusafe.2014.03.001>, URL <http://www.sciencedirect.com/science/article/pii/S0167473014000198>, Engineering Analyses with Vague and Imprecise Information.
- [16] A. Suksuwan, S. Spence, Optimization of uncertain structures subject to stochastic wind loads under system-level first excursion constraints: A data-driven approach, *Comput. Struct.* 210 (2018) 58–68, <http://dx.doi.org/10.1016/j.compstruc.2018.09.001>, URL <http://www.sciencedirect.com/science/article/pii/S0045794917314566>.
- [17] A. Beck, W. Gomes, R. Lopez, L. Miguel, A comparison between robust and risk-based optimization under uncertainty, *Struct. Multidiscip. Optim.* 52 (3) (2015) 479–492, <http://dx.doi.org/10.1007/s00158-015-1253-9>.
- [18] G. Schuëller, H. Jensen, Computational methods in optimization considering uncertainties – an overview, *Comput. Methods Appl. Mech. Engrg.* 198 (1) (2008) 2–13, <http://dx.doi.org/10.1016/j.cma.2008.05.004>.
- [19] D. Jerez, H. Jensen, M. Valdebenito, M. Misraji, F. Mayorga, M. Beer, On the use of directional importance sampling for reliability-based design and optimum design sensitivity of linear stochastic structures, *Probabilistic Eng. Mech.* 70 (2022) 103368, <http://dx.doi.org/10.1016/j.probenmech.2022.103368>, URL <https://www.sciencedirect.com/science/article/pii/S0266892022001011>.
- [20] P. Bjerager, Probability computation methods in structural and mechanical reliability, in: W. Liu, T. Belytschko (Eds.), *Mechanics of Probabilistic and Reliability Analysis*, Elme Press International, Lausanne, Switzerland, 1989, pp. 48–67.
- [21] Y. Wu, Computational methods for efficient structural reliability and reliability sensitivity analysis, *AIAA J.* 32 (8) (1994) 1717–1723.
- [22] K. Marti, Differentiation of probability functions: The transformation method, *Comput. Math. Appl.* 30 (3–6) (1995) 361–382.
- [23] S. Song, Z. Lu, H. Qiao, Subset simulation for structural reliability sensitivity analysis, *Reliab. Eng. Syst. Saf.* 94 (2) (2009) 658–665, <http://dx.doi.org/10.1016/j.res.2008.07.006>.
- [24] I. Papaioannou, K. Breitung, D. Straub, Reliability sensitivity estimation with sequential importance sampling, *Struct. Saf.* 75 (2018) 24–34, <http://dx.doi.org/10.1016/j.strusafe.2018.05.003>, URL <http://www.sciencedirect.com/science/article/pii/S0167473017304459>.
- [25] I. Papaioannou, K. Breitung, D. Straub, Reliability sensitivity analysis with Monte Carlo methods, in: B.E. G. Deodatis, D. Frangopol (Eds.), *11th International Conference on Structural Safety and Reliability, ICOSSAR*, New York, NY, USA, 2013, pp. 5335–5342.
- [26] H. Jensen, F. Mayorga, M. Valdebenito, Reliability sensitivity estimation of nonlinear structural systems under stochastic excitation: A simulation-based approach, *Comput. Methods Appl. Mech. Engrg.* 289 (2015) 1–23, <http://dx.doi.org/10.1016/j.cma.2015.01.012>, URL <http://www.sciencedirect.com/science/article/pii/S0045782515000250>.
- [27] H. Jensen, F. Mayorga, C. Papadimitriou, Reliability sensitivity analysis of stochastic finite element models, *Comput. Methods Appl. Mech. Engrg.* 296 (2015) 327–351, <http://dx.doi.org/10.1016/j.cma.2015.08.007>, URL <http://www.sciencedirect.com/science/article/pii/S0045782515002613>.
- [28] S. Au, Reliability-based design sensitivity by efficient simulation, *Comput. Struct.* 83 (14) (2005) 1048–1061.
- [29] J. Ching, Y. Hsieh, Local estimation of failure probability function and its confidence interval with maximum entropy principle, *Probabilistic Eng. Mech.* 22 (1) (2007) 39–49.
- [30] S. Chakraborty, B. Roy, Reliability based optimum design of tuned mass damper in seismic vibration control of structures with bounded uncertain parameters, *Probabilistic Eng. Mech.* 26 (2) (2011) 215–221.
- [31] H. Jensen, M. Valdebenito, G. Schuëller, D. Kusanovic, Reliability-based optimization of stochastic systems using line search, *Comput. Methods Appl. Mech. Engrg.* 198 (49–52) (2009) 3915–3924.
- [32] M. Valdebenito, G. Schuëller, Efficient strategies for reliability-based optimization involving non linear, dynamical structures, *Comput. Struct.* 89 (19–20) (2011) 1797–1811.

- [33] Z. Lu, S. Song, Z. Yue, J. Wang, Reliability sensitivity method by line sampling, *Struct. Saf.* 30 (6) (2008) 517–532, <http://dx.doi.org/10.1016/j.strusafe.2007.10.001>.
- [34] I.-W. Lee, G.-H. Jung, An efficient algebraic method for the computation of natural frequency and mode shape sensitivities - part I. Distinct natural frequencies, *Comput. Struct.* 62 (3) (1997) 429–435, [http://dx.doi.org/10.1016/S0045-7949\(96\)00206-4](http://dx.doi.org/10.1016/S0045-7949(96)00206-4), URL <http://www.sciencedirect.com/science/article/pii/S0045794996002064>.
- [35] C. Schenk, G. Schuëller, *Uncertainty Assessment of Large Finite Element Systems*, Springer-Verlag, Berlin/Heidelberg/New York, 2005.
- [36] G. Stefanou, The stochastic finite element method: Past, present and future, *Comput. Methods Appl. Mech. Engrg.* 198 (9–12) (2009) 1031–1051.
- [37] A. Chopra, *Dynamics of Structures: Theory and Applications to Earthquake Engineering*, Prentice Hall, 1995.
- [38] F.Y. Cheng, *Matrix Analysis of Structural Dynamics*, CRC, 2000, p. 992.
- [39] H. Jensen, M. Valdebenito, Reliability analysis of linear dynamical systems using approximate representations of performance functions, *Struct. Saf.* 29 (3) (2007) 222–237.
- [40] W. Gautschi, *Numerical Analysis*, second ed., Birkhäuser Boston, 2012, <http://dx.doi.org/10.1007/978-0-8176-8259-0>.
- [41] G. Schuëller, H. Pradlwarter, Benchmark study on reliability estimation in higher dimensions of structural systems – an overview, *Struct. Saf.* 29 (2007) 167–182.
- [42] A. Der Kiureghian, The geometry of random vibrations and solutions by FORM and SORM, *Probabilistic Eng. Mech.* 15 (1) (2000) 81–90.
- [43] P. Bjerager, Probability integration by directional simulation, *J. Eng. Mech.* 114 (8) (1988) 1285–1297.
- [44] R. Melchers, Importance sampling in structural systems, *Struct. Saf.* 6 (1) (1989) 3–10.
- [45] O. Ditlevsen, P. Bjerager, R. Olesen, A. Hasofer, Directional simulation in Gaussian processes, *Probabilistic Eng. Mech.* 3 (4) (1988) 207–217, [http://dx.doi.org/10.1016/0266-8920\(88\)90013-6](http://dx.doi.org/10.1016/0266-8920(88)90013-6), URL <http://www.sciencedirect.com/science/article/pii/0266892088900136>.
- [46] J. Nie, B. Ellingwood, Directional methods for structural reliability analysis, *Struct. Saf.* 22 (3) (2000) 233–249.
- [47] A. Ang, W. Tang, *Probability Concepts in Engineering: Emphasis on Applications to Civil and Environmental Engineering*, Wiley, 2007.
- [48] H. Flanders, Differentiation under the integral sign, *Am. Math. Mon.* 80 (6) (1973) 615–627, URL <http://www.jstor.org/stable/2319163>.
- [49] X. Yuan, S. Liu, M.A. Valdebenito, M.G. Faes, D.J. Jerez, H.A. Jensen, M. Beer, Decoupled reliability-based optimization using Markov chain Monte Carlo in augmented space, *Adv. Eng. Softw.* 157–158 (2021) 103020, <http://dx.doi.org/10.1016/j.advengsoft.2021.103020>, <https://www.sciencedirect.com/science/article/pii/S0965997821000491>.
- [50] A. Zerva, *Spatial Variation of Seismic Ground Motions – Modeling and Engineering Applications*, CRC Press, 2009.
- [51] L. Zhang, Dirac delta function of matrix argument, *Internat. J. Theoret. Phys.* (2020) URL <https://doi.org/10.1007/s10773-020-04598-8>.
- [52] I. Elishakoff, *Probabilistic Theory of Structures*, Dover Publications, New York, 1999.
- [53] R. Nelson, Simplified calculation of eigenvector derivatives, *AIAA J.* 14 (9) (1976) 1201–1205.